

**COMPUTATIONAL MICROBIOME ANALYSIS: METHODS AND  
APPLICATIONS**

(Spine title: Computational microbiome analysis: methods and applications)  
(Thesis format: Integrated Article)

by

**Ruth Wong**

Graduate Program in Biochemistry

A thesis submitted in partial fulfillment  
of the requirements for the degree of  
Masters of Science

The School of Graduate and Postdoctoral Studies  
The University of Western Ontario  
London, Ontario, Canada

© Ruth Grace Wong 2016

THE UNIVERSITY OF WESTERN ONTARIO  
School of Graduate and Postdoctoral Studies

**CERTIFICATE OF EXAMINATION**

Supervisor:

.....  
Dr. Gregory B. Gloor

Examiners:

.....  
Dr. Patrick O'Donoghue

Supervisory Committee:

.....  
Dr. Lindi M. Wahl

.....  
Dr. Chris J. Brandl

.....  
Dr. David R. Edgell

.....  
Dr. Jeremy Burton/Gregory Thorn

The thesis by

**Ruth Grace Wong**

entitled:

**Computational microbiome analysis: methods and applications**

is accepted in partial fulfillment of the  
requirements for the degree of  
Masters of Science

.....  
Date

.....  
Chair of the Thesis Examination Board

## Abstract

With the advent of next generation sequencing, scientists can obtain a more comprehensive snapshot of the bacterial composition of the microbiome, what genes they have, and what proteins they produce. We are in a phase of developing the experiments and accompanying statistical techniques to investigate the exact mechanisms by which the human microbiome affects health and disease. In this thesis we explore alternatives to the standard weighted and unweighted UniFrac metric for measuring the difference between microbiome samples, to extract different trends and outliers. We also apply next generation sequencing and computational analysis techniques to gut microbiome data to examine the relationship of the microbiota to non alcoholic fatty liver disease.

**Keywords:** Human microbiome, next generation sequencing, bioinformatics, non-alcoholic fatty liver disease

# Contents

<b>Certificate of Examination</b>	<b>ii</b>
<b>Abstract</b>	<b>iii</b>
<b>List of Figures</b>	<b>vi</b>
<b>List of Tables</b>	<b>vii</b>
<b>List of Appendices</b>	<b>viii</b>
<b>1 Introduction</b>	<b>1</b>
1.1 The human microbiome . . . . .	1
1.2 Exploring the human microbiome . . . . .	2
1.3 Illumina next generation sequencing platform . . . . .	2
1.4 Gene tag abundance . . . . .	3
1.4.1 16S rRNA gene sequencing experiment . . . . .	3
1.4.2 Operational Taxonomic Units . . . . .	4
1.4.3 General protocol and rationale . . . . .	4
1.4.4 Data analysis . . . . .	7
1.5 The metagenomic experiment . . . . .	9
1.5.1 Sequencing . . . . .	10
1.5.2 Imputation . . . . .	13
1.5.3 Data analysis . . . . .	13
1.6 Points of failure . . . . .	15
1.6.1 Collection methods differ . . . . .	15
1.6.2 Microbiome data is highly variable between individuals . . . . .	15
1.6.3 Microbiome data involves the comparison of many features . . . . .	16
1.6.4 Microbiome data is compositional . . . . .	16
1.6.5 Microbiome data is sparse . . . . .	18
1.7 The gut microbiome in patients with non-alcoholic steatohepatitis compared to healthy controls . . . . .	18
<b>2 Expanding the UniFrac toolbox</b>	<b>20</b>
2.0.1 Data . . . . .	22
2.0.2 Compositional Data Analysis . . . . .	22
2.0.3 Unweighted UniFrac . . . . .	23

2.0.4	Weighted UniFrac . . . . .	24
2.0.5	Analytical techniques . . . . .	25
2.0.6	Data preparation . . . . .	27
2.0.7	Unweighted Unifrac is highly sensitive to rarefaction instance . . . . .	29
2.0.8	The cause of rarefaction variation by Unweighted Unifrac . . . . .	32
2.0.9	Information UniFrac . . . . .	33
2.0.10	Tongue and buccal mucosa comparison . . . . .	34
2.0.11	Breast milk Data . . . . .	36
2.0.12	Monoculture data . . . . .	38
<b>3</b>	<b>The human microbiome and non-alcoholic fatty liver disease</b>	<b>41</b>
3.1	Introduction . . . . .	41
3.1.1	NASH progression risk . . . . .	41
3.1.2	Data . . . . .	42
3.1.3	Literature . . . . .	43
3.2	Methods . . . . .	45
3.2.1	16S rRNA gene tag experiment . . . . .	45
3.2.2	MetaPhlAn . . . . .	46
3.2.3	Metagenomic experiment . . . . .	46
3.3	Results . . . . .	48
3.3.1	16S rRNA gene tag experiment . . . . .	48
3.3.2	Metagenomic experiment . . . . .	57
3.4	Discussion . . . . .	62
<b>4</b>	<b>Theorems</b>	<b>63</b>
4.1	Basic Theorems . . . . .	63
<b>Bibliography</b>		<b>64</b>
<b>A</b>	<b>Workflows</b>	<b>71</b>
A.1	Non-alcoholic fatty liver disease metagenomic workflow . . . . .	71
A.1.1	Filter OTUs . . . . .	71
A.1.2	Get reference library genomes . . . . .	71
A.1.3	Get reference library coding sequences . . . . .	72
A.1.4	Annotate reference library coding sequences . . . . .	72
A.1.5	Map sequenced reads to reference library . . . . .	72
<b>Curriculum Vitae</b>		<b>73</b>

# List of Figures

1.1	<b>16S rRNA gene tag experiment workflow.</b> This shows the workflow from sample collection to data generation. The end result is a count table of reads per operational taxonomic unit per sample. . . . .	6
1.2	<b>Unweighted UniFrac.</b> When two samples do not share any branches of the phylogenetic tree, the unweighted UniFrac distance is maximized at 1. When two samples share half of their branch lengths on the phylogenetic tree, the unweighted UniFrac distance is 0.5. If the two samples contain exactly the same taxa, the unweighted UniFrac distance is minimized at 0, since the samples share all branches. . . . .	8
1.3	<b>Metagenomic experiment workflow.</b> This shows the workflow from sample collection to data generation. The end result is a table of number of sequencing reads per functionally annotated gene per sample. . . . .	12
1.4	<b>Example of stripcharts for subsystem 2 and 3 functional categorizations.</b> Dots on the left side are subsystem 4 annotations found to be more abundant in the healthy condition while dots on the right side are subsystem 4 annotations found to be more abundant in the bacterial vaginosis condition. Colored dots were found to be significantly differentially abundant. Figure taken from [54]. .	14
2.1	<b>Unweighted UniFrac.</b> When two samples do not share any branches of the phylogenetic tree, the unweighted UniFrac distance is maximized at 1. When two samples share half of their branch lengths on the phylogenetic tree, the unweighted UniFrac distance is 0.5. If the two samples contain exactly the same taxa, the unweighted UniFrac distance is minimized at 0, since the samples share all branches. . . . .	24



2.6	<b>Analysis of tongue and buccal mucosa data using different UniFrac weightings.</b> A principal component analysis of a 16S rRNA gene tag experiment done on samples from the tongue and buccal mucosa, selected from the Human Microbiome Project [95]. All weightings and the Bray-Curtis dissimilarity show separation between the samples by body site. Note that the variance explained by the first and second principal component axis is higher than in the tongue-tongue data set from Figure 2, which had 16.1% and 9.8% variance explained, respectively. . . . .	35
2.7	<b>Analysis of simulated monocultures using different UniFrac weightings.</b> A principal component analysis of a simulated 16S rRNA gene tag experiment based on the breast milk data. Red samples are dominated at 07% by <i>Pasteurella</i> , black samples are dominated by <i>Staphylococcus</i> , and cyan samples are dominated by <i>Pseudomonas</i> . Note that while information Unifrac appears to separate the samples reasonably well visually, the amount of variance explained by the first two components is much lower than even weighted UniFrac. . . . .	37
2.8	<b>Analysis of simulated monocultures using different UniFrac weightings.</b> A principal component analysis of a simulated 16S rRNA gene tag experiment based on the breast milk data. Red samples are dominated at 97% by <i>Pasteurella</i> , black samples are dominated by <i>Pseudomonas</i> , and cyan samples are dominated by <i>Staphylococcus</i> . Note that while information Unifrac appears to separate the samples reasonably well visually, the amount of variance explained by the first two components is much lower than even weighted UniFrac. . . . .	39
3.1	<b>Venn diagram of genera found to be differentially abundant by different studies between NASH/NAFLD and healthy controls.</b> Only 3 out of the 16 genera claimed to be differentially abundant were found in two studies: members of the <i>Escherichia</i> genus were found in the Zhu [102] and Jiang [40] studies, and members of the <i>Lactobacillus</i> and <i>Oscillibacter</i> genus were found in the Jiang [40] and Raman [75] studies. . . . .	44
3.2	<b>16S rRNA gene tag sequencing per sample bar plot.</b> Each column of this bar plot represents one sample, and each color represents one bacterial genus. Genus are listed in the legend in order of decreasing total abundance across all samples. Samples do not cluster according to their condition (healthy, simple steatosis, or nonalcoholic steatohepatitis). Note that OTUs that mapped to unclassified or <i>Incertae Sedis</i> were removed, and these made up just over a third of the total abundance. . . . .	49
3.3	<b>Principal Components Analysis of 16S rRNA gene tag sequencing data with different UniFrac weightings.</b> Each point represents one sample, and the distances between the samples have been calculated using different UniFrac metrics, taking into account phylogenetic as well as abundance information. There is no obvious separation between groups by any of the UniFrac weightings. Furthermore the variance explained by each principal component axis is not notably high, indicating a rather uniform data set. . . . .	50

3.4	<b>16S rRNA gene tag sequencing experiment biplot.</b> Compositional data analysis is done by transforming the counts with a centered log ratio transform, and then performing a principal coordinate analysis. The variance explained by each genus is overlayed on the same principal coordinate analysis plot. Note that the variance explained by the first and the second coordinate is 9% and 8% respectively, indicating that there is not a clear unidirectional separation between groups. Samples from healthy controls are colored black while samples from patients with NASH are colored red. . . . .	51
3.5	<b>Difference within vs. difference between groups.</b> Each point represents one OTU, and the differential abundance of that OTU within groups is plotted against the differential abundance between groups. None of the OTUs are more different between groups than within groups. The healthy samples used for these comparisons are the 10 healthy samples used for the metagenomic study. The extreme NASH samples used for these comparisons are the subset of the NASH patients selected for the metegenomic study. . . . .	52
3.6	<b>Correlation in effect sizes of different group experiments.</b> Each point represents one OTU, and the effect size of that OTU in one comparison (for example, comparing the gut microbiome of healthy patients with patients who have simple steatosis) is plotted against the effect size of that OTU in another comparison. The healthy samples used for these comparisons are the 10 healthy samples used for the metagenomic study. The extreme NASH samples used for these comparisons are the subset of the NASH patients selected for the metegenomic study. The median difference in the absolute effect sizes is -0.005547 for Healthy vs. NASH - Healthy vs. SS, 0.01094 for Healthy vs. extreme NASH - Healthy vs. SS, and 0.03105 for Healthy vs. extreme NASH - Healthy vs. NASH. The top decile of OTUs relatively increased in NASH for the metagenomic experiment are colored pink, and the top decile of OTUs relatively increased healthy for the metagenomic experiment are colored blue. . . . .	53
3.7	<b>Taxa barplot dendrogram derived from MetaPhlAn.</b> The metagenomic reads were input into MetaPhlAn to generate a count table. The taxa in the count table were filtered such that only taxa with at least 1% abundance in any sample was kept. In this barplot, each bar represents one sample, and each color represents one genus, with the size of the colored segments corresponding with the relative abundance of the genus. . . . .	58
3.8	<b>Biplot derived from MetaPhlAn.</b> Compositional data analysis is done by transforming the counts with a centered log ratio transform, and then performing a principal coordinate analysis. The variance explained by each genera is overlayed on the same principal coordinate analysis plot. This biplot was generated from the count table inferred by MetaPhlAn, with taxa filtered such that only taxa with at least 1% abundance in any sample was kept. Note that the variance explained by the first and the second coordinate is 17% and 11% respectively, indicating that there is not a clear unidirectional separation between groups. Samples from healthy controls are colored black while samples from patients with NASH are colored red. . . . .	59



# List of Tables

2.1	<b>Original abundance of taxa and rarefied abundance of taxa.</b> This data was simulated to demonstrate how rarefaction can change the distances reported by the unweighted UniFrac metric. The OTU in bold has been rarified to a zero count in sample A for one instance and a non zero count in the other instance. In Rarefaction 1, the unweightd UniFrac distance (unshared over total branches) is 0.4175, while in Rarefaction 2 the distance is 1.12. . . . .	33
3.1	<b>List of overall study inclusion and exclusion criteria.</b> This table lists the inclusion and exclusion criteria for the 16S rRNA gene tag experiment. . . . .	47
3.2	<b>List of inclusion and exclusion criteria for metagenomic study.</b> Patients were selected for the metagenomic study out of the patients selected for the 16S rRNA gene tag sequencing study with the following criteria. Ten healthy and ten patients with NASH were selected in total. . . . .	48
3.3	<b>Top decile of OTUs relatively increased in NASH based on effect size from healthy vs. NASH comparison.</b> This table lists the OTUs, their effect sizes in all the comparisons, as well as the corresponding genus-level effect sizes in the 16S rRNA gene tag experiment and MetaPhlAn comparisons between the 10 healthy and 10 NASH samples selected for the metagenomic study. The OTUs were picked by open reference, by clustering and comparison with the SILVA database [74]. Positive effect sizes indicate that the feature was found to be relatively increased in NASH while negative effect sizes indicate that the featuer was found to be relatively increased in healthy. OTUs were annotated with SILVA, and a confidence percentage is reported based on the provided bootstrapping algorithm. <i>Incertae Sedis</i> and unclassified genera were not analyzed at the genus level. . . . .	55



# **List of Appendices**

71Appendix.a.A

# **Chapter 1**

## **Introduction**

This thesis focuses on the human microbiome, its relation to human diseases, and techniques used in the data analysis and exploration of it. During the course of my thesis, I conducted one study about non-alcoholic fatty liver disease, and wrote a conference paper about alternate weightings of a common microbiome analysis technique (UniFrac). Each of these topics is represented as a chapter of my thesis.

### **1.1 The human microbiome**

Approximately half of the cells that make up the human body are bacterial [82]. Trillions of these bacteria live in the gut [36], and have a massive metabolic potential. For example, the gut microbiome has been shown to produce changes in hormone levels [56], short chain fatty acid levels [93], and ethanol levels [44], to name a few. The human gut microbiome can even digest polysaccharides otherwise unusable by humans [28].

This massive metabolic potential produces measurable symptomatic effects. Transplanting gut bacteria from obese mice to lean mice have been shown to convert lean mice to absorb more calories from the same food [92]. The microbiome can also affect behavior: Completely germ free mice exhibit more anxiety-like behaviors than specific pathogen free mice [62].

The human microbiome opens up a host of possibilities for reducing the effects of disease and improving quality of life. However, until recently, a deep understanding of the human microbiome has been beyond the reach of available technology. For example, *Escherichia coli* is a common model gut bacteria because it is easy to culture, however in reality only makes up about 1% of the average human gut microbiome [4].

With the advent of next generation sequencing, scientists can obtain a more comprehensive snapshot of the bacterial composition of the microbiome, what genes they have, and what proteins they produce [20]. We are in a phase of developing the experiments and accompanying statistical techniques to elucidate the exact mechanisms by which the human microbiome affects health and disease. Armed with a deeper understanding of how the microbiome works, we may be able to develop probiotic techniques to improve quality of life.

## 1.2 Exploring the human microbiome

The advent of next generation sequencing has prompted the development of a number of different experiments that can be run on biological samples of the human microbiome. Samples can be collected by swabbing the target body site or collecting excretions such as saliva or stool. Products such as DNA or RNA may be extracted as appropriate for the analysis.

Usually a study involves an experimental group and a control group. These can be patients with disease and healthy controls [54], people who are susceptible and resistant to a condition [89], or patients before and after a medical intervention [35]. The questions that scientists in this field generally want to answer are: Is the human microbiome driving or associated with the difference between the two groups? If so, what is the mechanism of action? There are also exploratory studies which try to determine what the core microbiome for a body site in a single condition is by examining what people who fit the condition have in common.

The questions that the data can answer directly are: Is there a statistically significant difference in the microbiome between the control and the experimental groups, in terms of the types of microbes present or the microbial genes present? Do separated groups exist in the data? Are the proportional abundances of certain taxa or genes correlated with each other, or with patient metadata? These questions can be answered by metagenomic experiments and statistical analysis, leading to clues about the larger questions of the mechanism of action.

The two metagenomic experiments that can be done with microbiome next generation sequencing data used in this thesis are gene tag abundance and deep metagenomic sequencing [76]. The tag used for gene tag abundance here is the 16S rRNA gene [33]. The process and resulting data of each experiment is described in the next section, followed by a piece about data analysis and points of failure.

## 1.3 Illumina next generation sequencing platform

Illumina is a next generation sequencing platform. The Illumina MiSeq machines yields up to 25 million reads of paired end 300 nucleotide sequences, and the Illumina HiSeq machines yield up to 4 billion reads of paired end 125 nucleotide sequences, as stated on the official Illumina website (<http://www.illumina.com/systems.html>). The sequencing works as follows:

1. DNA is amplified or fragmented to smaller pieces
2. Adaptors are ligated to the ends of the DNA
3. The DNA is denatured into single strands
4. The DNA washed on a flow cell covered in primers, such that complementary DNA sticks
5. The DNA on the flow cell is replicated to form clusters of identical sequences
6. The DNA is made single stranded again
7. Primers, nucleotides, DNA polymerase, and fluorescently labelled nucleotide terminators are added

8. A camera can detect the fluorescently labelled nucleotide terminators for each added base on each cluster of identical sequences, allowing the DNA to be sequenced.

The Illumina technology has been used for years [6], and standard protocols exist for library preparation, with kits available commercially.

## 1.4 Gene tag abundance

Gene tag abundance experiments provide an estimate of the proportion of different types of bacteria in the sample. This can be used to answer questions such as:

*What bacterial taxa make up the microbial community?* Scientists often want to characterize microbiomes for certain conditions. For example, the core gut microbiome was described by one group to have three enterotypes [4], however, when another group studied a diverse population including non-Western people, the enterotypes did not hold [101]. The vaginal microbiome is known to be Lactobacillus dominated, except in bacterial vaginosis, where the microbiome is much more diverse [39]. The idea is that characterizing the core microbiome is can lead to insight on core functions and how they can be altered when the core microbiome is disrupted.

*Are there any differentially abundant taxa between conditions?* Some theories of disease progression include the involvement of bacteria as pathogens. Others involve bacteria as probiotics, preventing disease progression. Salient examples include atopic dermatitis where flare-ups are associated with an increase in the proportion of *Staphylococcus aureus* on the skin [43], and RePOOPulate, a probiotic therapy where 33 microbes cultured from a healthy donor were used to successfully treat symptoms of *C. difficile* [71].

Historically, Koch's postulates have been used to determine if a microbe is a disease-causing pathogen: First, the microbe must be present in all cases of the disease. Second, the microbe must not be present and non-pathogenic in other diseases. Third, if the microbe is isolated in pure culture, it can be used to induce the disease [42]. One group has created a modified set of postulates that takes DNA sequencing into account [29] which can be applied to differentially abundant taxa detected by gene tag sequencing. However, Koch's postulates do not account for when the same bacteria can have a very different expression profile in health and disease, such as Lactobacillus iners in bacterial vaginosis [54].

*Do samples from different conditions cluster together?* Sometimes when the data is plotted, there appears to be separation between groups, even if specific taxa are not differentially abundant. One example of this is a study on discordant gut microbiomes between twins in Malawi where one twin has kwashiorkor and the other is healthy [85]. In this case the microbiomes diverge the most during treatment with ready-to-use therapeutic food.

### 1.4.1 16S rRNA gene sequencing experiment

The gene tag chosen throughout this thesis is the gene for the 16S subunit of ribosomal RNA. The 16S rRNA gene is present in all known bacteria and has regions of variability interspersed with regions of high conservation. This allows primers to be made to match the conserved regions, such that the variable regions can be amplified, sequenced, and used to infer taxa.

Entire databases exist specifically to match the 16S rRNA gene with taxonomy, such as SILVA [74], the Ribosomal Database Project [16], and Greengenes [19].

Specifically, we have been using the 16S rRNA gene primers from the Earth Microbiome Project protocol [31], which amplify the V4 variable region of the 16S rRNA gene. This region was identified by PrimerProspector to be nearly universal to archaea and bacteria [97].

### 1.4.2 Operational Taxonomic Units

Unlike more distinct species, such as mammalian species, bacterial species are not well defined. Bacterial genomes are highly variable, and regions used to identify bacteria vary in a continuum rather than clusters of similar sequences.

Historically bacteria that are have 97% identity in a variable region are considered to be the same taxa. The 97% cutoff was arbitrarily chosen to best map sequence data to bacterial classifications. This threshold maximizes the grouping of bacteria classified as the same species while minimizing the grouping of bacteria classified as different species. Before sequencing bacterial classification was often done by appearance or by metabolic products, so there are outliers where bacteria classified in the same species are actually genetically very different, or bacteria classified in different genus are genetically very similar.

However, it is difficult to determine how a batch of sequences should be partitioned into groups of 97% identity. One way is to perform a clustering algorithm that optimally partitions the groups and then later assign taxonomic identity by matching the sequences with public databases. Another way is to start off with seed sequences from known bacteria and perform the clustering such that the 97% identity groups are centered on the seed sequences. In any case, the resulting taxonomic groupings are known as Operational Taxonomic Units (OTUs), and are used consistently within the same experiment. While OTUs can be annotated with standard taxonomic names such that results can be compared between experiments, technically the taxonomic groupings used by different experiments are not the same.

### 1.4.3 General protocol and rationale

The 16S rRNA gene sequencing experiment uses next generation sequencing to estimate the proportional abundance of different bacterial taxa. Samples are extracted and prepared for sequencing, and then the sequenced reads are collated into counts per assumed taxa per sample. The resulting table undergoes statistical analysis.

#### Pre-sequencing processing

There are several very general steps to the pre-sequencing process:

1. Take a biological sample and extract the DNA The sample can be collected swabbing the target body site or by collecting samples in some other way. DNA extraction is usually done with common commercial kits.
2. Run a PCR amplification As discussed previously, the gene tag experiments in this thesis amplify the V4 region of the 16S rRNA gene, following the Earth Microbiome Project

protocol [12]. The set of primers that we use are barcoded, so that we can sequence all the samples in the same sequencing run and differentiate them afterwards.

3. Run sequencing We use 150 nucleotide paired-end sequencing on the Illumina MiSeq platform. The 150 nucleotide paired ends allow us to overlap paired sequences in the middle to reconstitute the full sequence of the variable region.

### **Post-sequencing processing**

Here are the steps for going from raw sequenced reads to a table of counts per taxa per sample.

1. Demultiplex the raw sequence The barcodes are used to separate the sequences according to what sample they came from.
2. Assemble the paired ends of sequenced DNA The paired sequences are overlapped in the middle, resulting in the full variable region amplified by the primers.
3. Group the reads into operational taxonomic units (OTUs) We used UCLUST to cluster the reads into groups of 97% identity [23].
4. Annotate the OTUs with bacterial taxonomy Annotation was done by matching our OTUs to the SILVA database [74].
5. Generate a phylogenetic tree This can be done using the center-most sequence of each cluster that forms each OTU, and putting the sequences in a multiple sequence alignment, using software such as MUSCLE [22].

Alternatively, an Individual Sequence Unit (ISU) based approach rather than an OTU based approach can be taken, where the individual sequences are preserved even after grouping into OTUs, so that different strains within the same OTU can be analyzed separately [9].

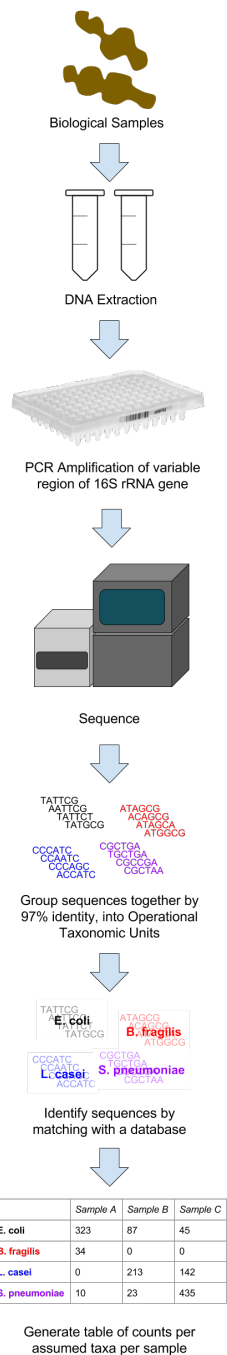


**Figure 1.1: 16S rRNA gene tag experiment workflow.** This shows the workflow from sample collection to data generation. The end result is a count table of reads per operational taxonomic unit per sample.

### 1.4.4 Data analysis

There are two goals in gene tag data analysis. First, is there any structure in the data (separation, clustering, correlations, differentials, etc.)? Second, what drives the structure in the data?

Separation or clustering can be examined by determining the distance between each sample, and using these distances to plot the samples as points on a graph. The following sections will go over the most commonly used distance metric in microbiome research, called UniFrac, as well as the Principal Components Analysis multidimensional scaling method for plotting the points on a graph. Afterwards the data can be visually or mathematically inspected for separation or clustering.

The technique used for determining if taxa are differentially abundant between groups is the same technique used for determining if gene annotations are differentially abundant between groups in the metagenomic experiment, and has its own section, titled “Compositional data analysis”.

#### UniFrac

Principal Component Analysis is necessary for multivariate statistics, and It is well known that the Principal Component Analysis cannot be performed on proportions, such as the OTU abundances derived from gene tag sequencing. Instead, a Euclidean distance is required [3].

In 2005, Lozupone et al introduced the UniFrac distance metric, a measure to calculate the difference between microbiomes that incorporated phylogenetic distance [52]. The goal of UniFrac was to enable objective comparison between microbiome samples from different conditions. In 2007, Lozupone added a proportional weighting to the original unweighted method [51]. Since then, papers reporting these metrics have garnered over a thousand citations, and enabled research about everything from how kwashiorkor causes malnutrition [85] to how people can have similar microbiomes to their pet dogs [86]. Except for Generalized UniFrac, used to make hybrid unweighted and weighted UniFrac comparisons [14], few advances in the metric have occurred since 2007.

#### Unweighted UniFrac

Unweighted UniFrac uses an inferred evolutionary distance to measure similarity between samples. It requires a reference phylogenetic tree containing all the taxa present in the samples to be examined. The calculation is performed by dividing the branch lengths shared between the two samples by the branch lengths covered by either sample. A distance of 0 means that the samples have an identical set of taxa detected, and a distance of 1 means that the two samples share no taxa in common.

The qualitative rather than quantitative nature of unweighted UniFrac makes the metric very sensitive to sequencing depth. A greater sequencing depth generally results in the detection of a greater number of taxa. To account for this problem, ecologists use a technique called rarefaction to normalize the sequencing depth across samples by random sampling without replacement [13]. However, in unweighted UniFrac samples move relative to the other samples in different rarefaction instances, to the point where they can switch from being a member of one cluster of data to another, as demonstrated in the chapter Expanding the UniFrac Toolbox.

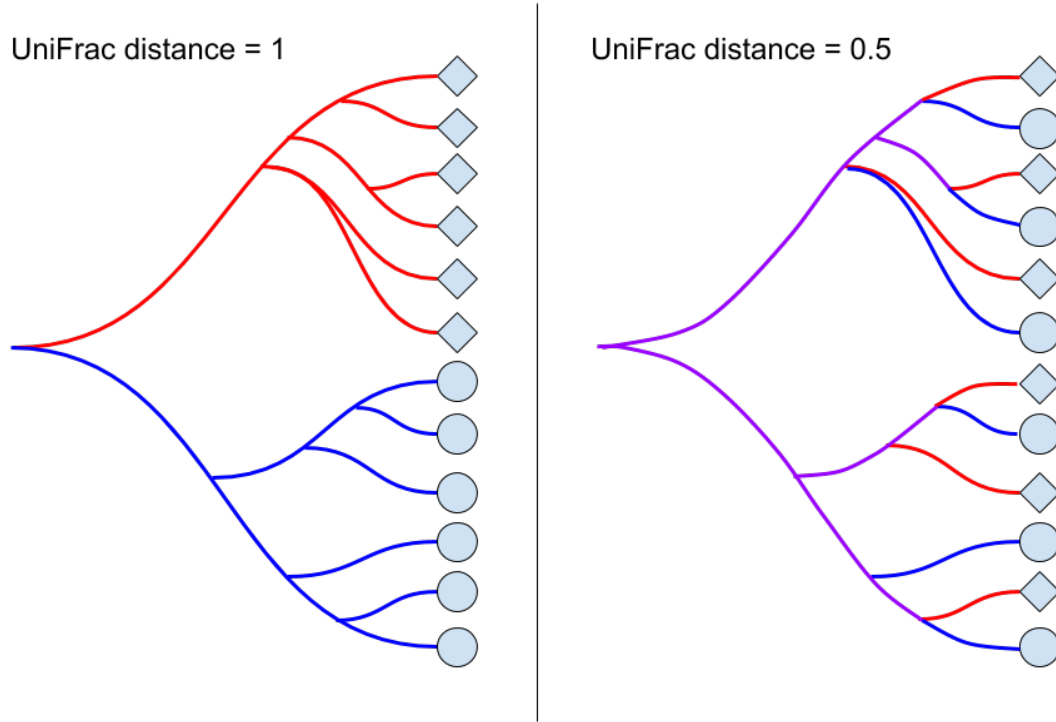


**Figure 1.2: Unweighted UniFrac.** When two samples do not share any branches of the phylogenetic tree, the unweighted UniFrac distance is maximized at 1. When two samples share half of their branch lengths on the phylogenetic tree, the unweighted UniFrac distance is 0.5. If the two samples contain exactly the same taxa, the unweighted UniFrac distance is minimized at 0, since the samples share all branches.

### Weighted UniFrac

Weighted UniFrac is an implementation of the Kantorovich-Rubinstein distance in mathematics, also known as the earth mover's distance [25]. Rather than looking only at the presence or absence of taxa, each branch length of the phylogenetic tree is weighted by the difference in proportional abundance of the taxa between the two samples. This technique reduces the problem of low abundance taxa being represented as a 0 or by a low count depending on sampling depth. In unweighted UniFrac, such taxa would flip from absent to present, and could skew the measurement: this would be especially problematic if the taxa are on a long branch. In weighted UniFrac, low abundance taxa have a much lower weight and so will have a lower impact on the total distance reported by the metric.

UniFrac is constituted as either a presence/absence (unweighted UniFrac) [52], a linear proportion in the form of weighted UniFrac [51], or some combination of the two in the form of Generalized UniFrac [14]. However, the data are not linear, because the sum of the total number

of reads is constrained by the sequencing machinery [30]. Alternative weightings and non-linear transformations of data need to be explored.

### Principal Components Analysis

Once the distances between each pair of samples has been calculated, they can be visualized on a plot, with each sample represented as one point. For visualization, the data should be placed so distances are preserved as much as possible, so that clustering and separation of samples can be clearly seen. This is done using the Principal Coordinate Analysis method of multidimensional scaling [21], shortened as PCoA.

To plot all of the samples as points in space such that the distances between each pair of samples are preserved, multiple dimensions are required. In this data specifically, the number of dimensions required is equal to one less than the number of samples. PCoA rescales all the dimensions as components, so that the first component captures the largest variation, or spread of the data, the second component captures the largest variation remaining in the data after the first component, and so on. This way, even if only the first two components are used to plot all the samples as points on a two dimensional graph, the data is spread out to enable visualization of separation or clustering.

After multidimensional scaling the data can be analyzed in several ways. The data can be examined for clustering by k-means analysis [90]. The points can also be measured for separation by looking only at their position on the first principal component axis, especially if the first axis covers the majority of the variation in the data set. With each sample associated with a number on the first principal component axis, one can examine the effect size of two different groups by taking the mean positions and dividing by the standard deviation.

## 1.5 The metagenomic experiment

Deep metagenomic sequencing provides an estimate of the proportion that each type of gene comprises out of the total genes present in the genetic material of the sample. This can be used to answer questions such as:

*What is the metabolic potential of the microbial community?* The metabolic potential is made up of all the protein functions that are coded by the genetic material present in the sample. Biologically speaking, these protein functions represent the enzymatic reactions that the microbiome could produce if all the genes were expressed. For example, the human gut microbiome has more genes related to methanogenesis, compared to the average sequenced microbe [32].

*Are any genes, functional categories of genes, or metabolic pathways made up of genes differentially abundant between groups?* In 2006, Turnbaugh et al published a paper showing that an obesity associated gut microbiome in mice had an increased capacity for energy harvest [92], sparking more research into the gut microbiome and obesity related ailments such as diabetes [47] and non-alcoholic fatty liver disease [102]. The ability to check if genes, functional categories of genes, or pathways are differentially abundant between groups allows scientists to find clues about the mechanisms by which the microbiome affects certain diseases.

All of this information can be determined by either imputation or actual sequencing, discussed in the next sections.

### 1.5.1 Sequencing

The goal of metagenomic analysis is to examine the metabolic potential of the microbiota in the microbiome. This is done by identifying genes, sorting them by the known function of the protein for which they code (such as the catalyzation of a certain reaction), and checking if any functions are differentially present between conditions. Further analysis can also include checking for pathway enrichment, and assembling the sequenced reads into genomes. The general protocol for metagenomic analysis is as follows:

1. Take a biological sample and perform DNA extraction The sample can be collected by swabbing the target body site or collecting excretions.
2. Prepare the DNA for sequencing Fragment the DNA, and filter for the desired size. These steps are all part of the standard Illumina library prep protocol for the HiSeq. There are two options for fragment size, either 50 or 100 nucleotides in length, and we chose the longer one for easier assembly and mapping.
3. Sequence the DNA. We performed single end sequencing on the Illumina HiSeq platform, with our samples barcoded so that they could be pooled into the same sequencing run.
4. Create an annotated library of reference sequences The annotated library contains annotations about what kind of protein each sequence codes for. The first step to creating the annotated library is to gather a database of sequences. The database of sequences can be created before the sequencing is complete by gathering all the genomes of all the bacterial strains predicted to be present in the sample, or it can be created after sequencing by assembling the sequenced reads into parts of genomes. The second step is to annotate the sequences with predicted protein functions. Some publically available genomes already have protein annotations. For genomes or partial genomes without annotations, the placement of genes can be predicted by looking for open reading frames, and these predicted genes can be aligned with databases such as SEED [65] or KEGG [41] to match them with functional annotations, using the BLAST algorithm [2].
5. Map the sequenced reads to the library. Mapping is the process of annotating the sequenced reads by aligning them with sequence that has already been annotated. We used Bowtie2 [46] to map our sequenced reads to the annotated library created in the previous step. Bowtie2 aligns similar sequences together.
6. Determine how many mapped reads match each functional annotation. Once the sequenced reads have been mapped to the annotated reference sequence, the number of reads sequenced for each annotation can be counted up. The end result is a table of counts per gene annotation per sample.

Issues with sequencing and the analysis of sequencing data arise from sampling and the fat nature of the data. The sequences that are read by the sequencer are only a small fraction of the DNA from the sample. Additionally, primers used for sequencing may be biased for certain sequences more than others. Lastly, the data is very fat, which is to say that there are magnitudes more variables (in the form of functional annotations of genes) than there are

samples. This makes it difficult to have enough power to detect small differences in the data, a concept expanded upon in the Points of Failure section below.

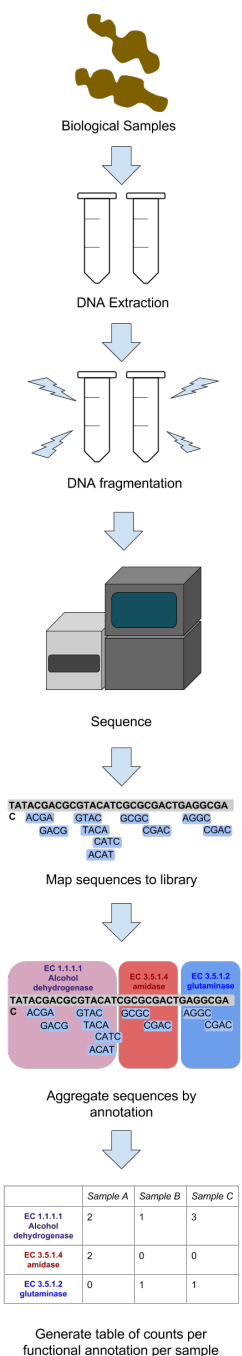


**Figure 1.3: Metagenomic experiment workflow.** This shows the workflow from sample collection to data generation. The end result is a table of number of sequencing reads per functionally annotated gene per sample.

## 1.5.2 Imputation

Deep metagenomic sequencing can be imputed using a tool called PiCrust from a gene tag experiment [45]. PiCrust uses the Greengenes database [19] to identify the bacterial taxa in the sample, and pulls their genomes from the Integrated Microbial Genomes database [57]. With the genomes, the program tries to predict what would be seen if the samples underwent deep metagenomic sequencing. For taxa without a fully sequenced genome, PiCrust infers the genetic content based on ancestors in the phylogenetic tree. PiCrust produces metagenome predictions with Spearman  $r= 0.7$  [45], compared to a full metagenomic sequencing experiment.

Imputation is useful for identifying potential correlations that should be explored and validated further, but should not be used to make conclusions. The issues with imputation include all the issues with sequencing, plus the added variation in its imperfect correlation.

## 1.5.3 Data analysis

Data analysis can be performed by seeing if functions are differentially abundant between samples in different groups (described in the “Compositional data analysis” section), examining functional categorizations, and checking for pathway enrichment.

### Functional categorization

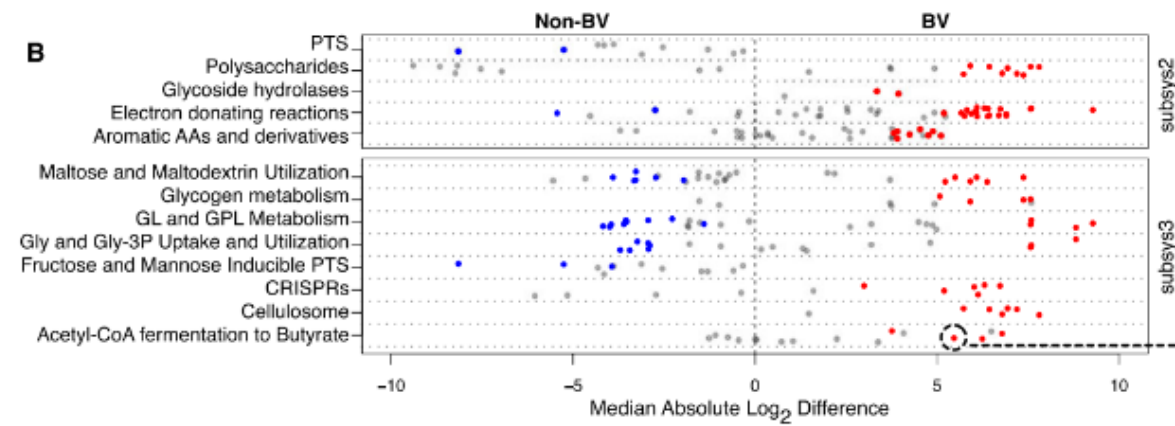


**Figure 1.4: Example of stripcharts for subsystem 2 and 3 functional categorizations.** Dots on the left side are subsystem 4 annotations found to be more abundant in the healthy condition while dots on the right side are subsystem 4 annotations found to be more abundant in the bacterial vaginosis condition. Colored dots were found to be significantly differentially abundant. Figure taken from [54].

We use the SEED annotation, which has four different levels of categorization. Subsystem 4 is the most atomic categorization level and describes the specific function of the protein group, for example, “Isovaleryl-CoA dehydrogenase (EC 1.3.99.10)”. Subsystem 3, 2, and 1 are increasing more general levels of categorizations, from enzyme families to large categorizations such as genes related to carbohydrate metabolism.

Even if the subsystem 4 functional categories are not significantly different between groups, they each have an effect size with a direction. Stripcharts can be used to plot the effect sizes of the subsystem 4 categories for a larger category. For example, by plotting the effect sizes of all the subsystem 4 categorizations under Carbohydrate Metabolism, one can visually see if there are any obvious directional trends for carbohydrate metabolism functions being more present in the experimental group compared to the control.

### Pathway enrichment

Biological pathways can be thought of as made up of a series of chemical reactions, each catalyzed by a protein enzyme, which is encoded by a gene. KEGG (Kyoto Encyclopaedia of Genes and Genomes) is a manually curated annotation database that matches genes to pathways [41]. This database allows researchers to see if there is differential abundance of pathways encoded by functionally annotated genes, even when the genes may not be differentially abundant by themselves.

## 1.6 Points of failure

The Huttenhower lab has organized the Microbiome Quality Control project (MBQC) at <http://www.mbgc.org/>. Preliminary results show that despite being given the same samples, different participating labs can come up with vastly different results. This lack of reproducibility is caused by a lack of consensus on the correct way to analyze microbiome data. The following sections explore different aspects of microbiome data that contribute to this.

### 1.6.1 Collection methods differ

These experiments are very sensitive to batch effects because microbiome composition can be very variable within groups such that the effect size of a difference between groups can be small. Wherever possible, all samples should be processed in the same batch. Analysis should also be done to check if samples extracted on different dates or sequenced with different primers separate into clusters, to make sure that there is no systematic bias in the data.

### 1.6.2 Microbiome data is highly variable between individuals

One highly studied body site is the gut, and the gut microbiome can be affected very strongly by diet [94]. This among other factors lead to a highly diverse gut microbiome between subjects for reasons unrelated to the disease being studied, creating a lot of noise, potentially obscuring real effects or even creating the appearance of false effects.

Generally experiments of this nature typically have low sample sizes due to budget constraints, sample collection difficulties, patient compliance, and other issues. To increase cost effectiveness and reduce batch effects, we run all the samples in an experiment on the same sequencing run, by means of a primer design [33].

There are several models for computationally analyzing the variance within conditions in order to determine if operational taxonomic units are significantly differentially abundant, most of which were originally designed for RNA-seq experiments on single organisms [66]. Currently

the most popular tools for analyzing differential abundance are EdgeR [78], DESeq2 [49], and MetagenomeSeq [69]. EdgeR was cited by 1,130 papers in 2015 according to Google Scholar. DESeq2 and MetagenomeSeq are part of the QIIME pipeline, which was cited by 1,620 papers in 2015.

EdgeR and DESeq2 use the negative binomial distribution. The negative binomial distribution allows the variance of data to be estimated given the mean, through a function. The function is determined by collecting the mean and variance for all the counts for each OTU in each experimental condition, and fitting the variances according to the negative binomial distribution. This vastly underestimates the variance at low counts, which represent the sampling of low abundance OTUs, and can be very different between replicates. Underestimating the variance at low counts produces spurious low p-values for low count OTUs [26].

MetagenomeSeq uses the Zero-Inflated Gaussian (ZIG) model, which is a binomial distribution of counts (that may include zero counts), plus a function to predict how many extra zeros there will be. This doesn't work well when the total number of reads are not well matched, because then there will be much more zeros in the data set with less reads, due to having a lower sequencing depth, and a consistent total read count is required between samples according to page 2 of the supplementary material in the first metagenomeSeq paper [69].

For my differential abundance analysis, I've used ALDEx2, which samples from the Dirichlet distribution to model variation in the data [27]. After a number of samples, the mean value and mean variance are used to determine if OTUs are differentially abundant between groups, an approach that is believed to result in greater sensitivity and equivalent specificity compared to the DESeq2 approach [27].

### 1.6.3 Microbiome data involves the comparison of many features

Oftentimes, the number of taxa or gene functions comparisons is a magnitude larger than the sample size. This is known in statistics as having more variables than observations, or having fat data. The higher the ratio of variables to observations are, the less likely the principal components analysis is to be reliable [64].

Researchers should include multiple test corrections to ensure that the results they are reporting are true, at the expense of having p-values less than 0.05. Unfortunately many studies have been published in high impact journals without multiple test corrections, including a famous paper linking the gut microbiome to autism published in Cell [38].

### 1.6.4 Microbiome data is compositional

In both gene tag sequencing and metagenomic sequencing experiments, the data is in the form of a list of counts per feature, with the features composing an aspect of the microbiome for each sample. This is compositional data. There are several core truths about microbiome data and its compositional nature that should be considered when making an analysis strategy.

First, the total number of reads per sample is irrelevant to the biological implications of the data. The number of reads is influenced by the sampling methodology (for example, the gut microbiome can be sampled by rectal swab or by fecal sample), the way the samples were processed, the quality of the DNA, the performance of the sequencing machine, as well as the bias in the specificity of the primers used for amplifying the DNA. The high amount of technical

variation from all of these sources mean that the total number of reads per sample cannot be used to make biological inferences.

Second, spurious correlations can arise from proportional microbiome data, and should be avoided. In the late 19th century, many studies were being published about how organ sizes (normalized by dividing the size by the individual's height) were correlated. However, it was discovered that when two sets of uncorrelated data are both divided by a third set of uncorrelated data, the two sets will appear spuriously correlated. This is analogous to microbiome data where raw counts are normalized by dividing by the total number of counts [70].

Additionally, the constrained sum causes the abundance of different taxa to appear to be negatively correlated with each other when analyzed by conventional statistics. When one taxa increases in abundance, the counts detected in other taxa decrease in abundance, even if the taxa are not decreasing in abundance biologically.

Third, removing an entire variable (an OTU in gene tag sequencing, or a functional annotation in deep metagenomic sequencing) from the analysis should not change correlations between OTUs. A correlation between two OTUs is suspect if it is dependant on the presence of an additional unrelated OTU. Removing variables occur routinely in microbiome research. For example, rare OTUs are thought to not be very informative, and low counts have such high variability, so they are often filtered out. Additionally, primers may be biased against certain taxa, which are underrepresented in the data. Finally, some experiments are performed only on taxa of interest (as is the case with qPCR), and all other OTUs are not considered in the analysis. Without a data transformation, removing variables from the full set will change the correlation between variables [1].

To ensure that these conditions are met, data should be analyzed in a compositional way. In Euclidean space, data points can increase or decrease freely. Compositional data is under a sum constraint, and exist in a non-Euclidean space known as the Aitchison simplex [1]. A data transformation can be performed to put the data into Euclidean space, so that it can be analyzed with standard statistical methods that depend on Cartesian coordinates and linear relationships.

Several types of log ratio data transformations are recommended to allow the data to be analyzed by standard Euclidean methods [1]. The type that makes the most sense for microbiome data is the centered log ratio transform. The centered log ratio transform is performed by dividing each proportional abundance by the geometric mean of all the proportional abundances, and taking the logarithm. Here  $x_i$  is one proportional abundance within a sample, and there are  $n$  OTUs in total.

$$clr(x_i) = \frac{x_i}{\sqrt[n]{\prod_{i=1}^n x_i}}$$

The geometric mean acts as a low level baseline abundance in microbiome data. Taking the logarithm of the ratio allows for a consistent measurement whether the large number is in the numerator or denominator of the ratio.

The centered log ratio transform prevents the total number of reads from affecting the measurement, so long as the geometric mean is a relatively stable baseline. The geometric mean is stable when the total number of reads is constant, or the per feature variation is random. The latter condition is met in a typical microbiome data set. The centered log ratio transform also

allows for coherent subcompositional data analysis as remaining values are not affected when entire variables are removed.

Compositional techniques such as those espoused in the ANOVA-Like Differential Expression 2 (ALDEx2) software [27] and the Analysis of Composition of Microbiomes (ANCOM) framework [55] should be used to promote consistent data analysis. ALDEx2 performs a log ratio transform and then models the technical variation using the Dirichlet distribution while ANCOM uses log ratio analysis to make point estimates of the variance and mean, without any distributional assumptions.

However, these techniques are not yet mainstream in the field, resulting in a high number of conclusions made that are not reproducible. One example of this is referenced in the chapter about the gut microbiome and non alcoholic fatty liver disease, where five papers have been published on the same topic with almost non overlapping results.

### 1.6.5 Microbiome data is sparse

One of the fundamental challenges in analyzing differential abundance is accounting for zeroes. Unlike a presence/absence test, a zero does not necessarily mean that the expression is not there. The expression could be present in an amount smaller than the resolution of the test, or it be present but missed due to random sampling. This is a problem because when statistical methods are used to examine significantly different expression, as the comparison of zero values to non-zero values are likely to come out as significant whether or not the expression is differential. However, a 0 and a 1 count are easily interchangeable between technical replicates and the difference is not biologically significant. Additionally, the log transformations used in compositional data analysis cannot be performed on zeros. Statisticians often recommend that any sample with at least one zero count be removed during compositional data analysis, but for microbiome data this would often result in the removal of all the samples [1].

The solution for dealing with the zeros in microbiome data is to add a small arbitrary value to each zero, as suggested in the original literature about the statistical analysis of compositional data [1]. Two methods have been suggested to do this. This is used in ALDEx2, and the arbitrary value (known as the prior in Bayesian terms) is chosen to be 0.5, representing complete uncertainty in whether or not a zero count in one sample (where the OTU or gene has non zero counts in other samples) would be a 0 or a 1 in a technical replicate [26].

The second method is to calculate likelihood that a zero could be changed to a positive count if the sample were resequenced is estimated, based on the within group variance of the counts of the feature. This is implemented by the cmultRepl command in the zCompositions package in R, with the ‘count multiplicative zeros’ option [67]. Based on the shape of the rest of the data for the same sample, the average value of the count detected if a zero were resequenced is determined (a posterior value in Bayesian terms), and the zeros are all replaced by this fraction.

The microbiome field is quite new, and has been undergoing many exciting developments. Gold standards must be set to ensure that studies are replicable, and that published research represents the biological reality.

## 1.7 The gut microbiome in patients with non-alcoholic steatohepatitis compared to healthy controls

Non alcoholic fatty liver disease (NAFLD) has been on the rise along with obesity, affecting a fifth to a third of the North American population [72]. Most people with NAFLD remain asymptomatic, however, in up to a third of patients NAFLD can progress to non-alcoholic steatohepatitis (NASH), causing inflammation and scarring in the liver, and decreasing the 5 year survival rate to 67% [73]. If we can shed some light on the process by which people progress from NAFLD to NASH, we might be able to find treatments to prevent NASH.

Several genetic [88] [77], epigenetic [61], hormonal [100], and metabolite [75] factors are known to affect the risk progression to NASH. The relationship between the gut microbiome and non alcoholic fatty liver disease is less clear.

A 2001 paper performed C-D-xylose-lactulose breath tests and measured tumor necrosis factor alpha levels to determine presence of bacterial overgrowth, and found increased bacterial overgrowth in 22 patients with NASH compared to 23 healthy controls [98]. Some papers claim a link between ethanol-producing gut bacteria and NAFLD [102] [40], however, no multiple test correction was performed in these studies. Five published studies claiming to have found differentially abundant bacteria in the gut microbiome between healthy controls and patients with non alcoholic fatty liver disease have nearly non-overlapping results [102] [99] [75] [40] [8].

These five studies do not form a consistent story about the gut microbiome and NAFLD. In one chapter of this thesis we report the results of our own analysis, which we have attempted to run rigorously, such that our results are replicable. Additionally, we are running a deeply sequenced metagenomic study, which hasn't been done in the past.

## **Chapter 2**

### **Expanding the UniFrac toolbox**

## Expanding the UniFrac toolbox

Ruth G Wong<sup>1</sup> , Jia R Wu<sup>1</sup> , Gregory B Gloor<sup>1</sup> 

**1 Department of Biochemistry, University of Western Ontario, London, Ontario, Canada**

 **These authors contributed equally to this work.**

\* [gloor@uwo.ca](mailto:gloor@uwo.ca)

## Abstract

The UniFrac distance metric is often used to separate groups in microbiome analysis, but requires a constant sequencing depth to work properly. Here we demonstrate that unweighted UniFrac is highly sensitive to rarefaction instance and to sequencing depth in uniform data sets with no clear structure or separation between groups. We show that this arises because of subcompositional effects. We introduce information UniFrac and ratio UniFrac, two new weightings that are not as sensitive to rarefaction and allow greater separation of outliers than classic unweighted and weighted UniFrac. With this expansion of the UniFrac toolbox, we hope to empower researchers to extract more varied information from their data.

## Introduction

In 2005, Lozupone et al introduced the UniFrac distance metric, a measure to calculate the difference between microbiomes that incorporated phylogenetic distance [52]. The goal of UniFrac was to enable objective comparison between microbiome samples from different conditions. In 2007, Lozupone added a proportional weighting to the original unweighted method [51]. Since then, papers reporting these metrics have garnered over a thousand citations, and enabled research about everything from how kwashiorkor causes malnutrition [85] to how people can have similar microbiomes to their pet dogs [86]. Except for generalized UniFrac, used to make hybrid unweighted and weighted UniFrac comparisons [14], few advances in the metric have occurred since 2007. In this paper we examine data sets where UniFrac gives misleading results, and present and discuss some alternative weightings for UniFrac.

## Operational Taxonomic Units

Unlike more distinct species, such as mammalian species, bacterial species are not well defined. Bacterial genomes are highly variable, and regions used to identify bacteria vary in a continuum rather than clusters of similar sequences.

Historically bacteria that are have 97% identity in a variable region are considered to be the same taxa [15]. The 97% cutoff was arbitrarily chosen to best map sequence data

to bacterial classifications. This threshold is thought to maximizes the grouping of bacteria classified as the same species while minimizing the grouping of bacteria classified as different species [10]. Before sequencing bacterial classification was often done by appearance or by metabolic products, so there are outliers where bacteria classified in the same species are actually genetically very different, or bacteria classified in different genus are genetically very similar.

However, it is difficult to determine how a batch of sequences should be partitioned into groups of 97% identity. One way is to perform a clustering algorithm (using software such as UCLUST [23]) that partitions the groups and then later assign taxonomic identity by matching the seed or central sequences with public databases, such as SILVA [74], the Ribosomal Database Project [16], or Greengenes [19]. Another method is closed reference OTU picking, which starts off with seed sequences from known bacteria and perform the clustering such that the 97% identity groups are centered on the seed sequences. In any case, the resulting taxonomic groupings are known as Operational Taxonomic Units (OTUs), and are used consistently within the same experiment. While OTUs can be annotated with standard taxonomic names such that results can be compared between experiments, technically the taxonomic groupings used by different experiments are not the same, except with closed reference OTUs, or individual sequence unit methods. Individual sequence unit (ISU) methods which do not use OTUs can be run with software such as DADA2 [9].

Grouping of amplicon sequences into OTUs allows for the data to be summarized into a table of counts per OTU per sample.

### 2.0.1 Data

UniFrac requires two pieces of information: phylogenetic tree and a table of counts per inferred taxa per sample. These are derived from a gene tag sequencing experiment, such as the commonly used 16S rRNA gene [91]. The sequenced gene contains a variable region, allowing the sequences to be grouped into OTUs as described in the previous section. A count table can then be generated with the number of reads per OTU per sample. The center sequence of each OTU group can be put into a multiple sequence alignment, from which a phylogenetic tree can be inferred.

The phylogenetic tree is created through a multiple sequence alignment with the representative OTU sequences, using software such as MUSCLE [22], or using a guide tree, such as through Greengenes [19] or the QIIME software [11]. Each leaf of the tree represents one of the OTUs, and each of the branches of the tree has a length. Additionally, the tree needs to be rooted for the UniFrac calculation to be performed. This is often done by rooting the tree at its midpoint.

### 2.0.2 Compositional Data Analysis

Microbiome data is in the form of a list of counts per feature (OTUs in this case), with the features composing an aspect of the microbiome for each sample. This is compositional data. There are several core truths about microbiome data and its compositional nature that should be considered when making an analysis strategy.

First, the total number of reads per sample is influenced by sample collection, extraction, sequencing library preparation, and sequencing platform, and is irrelevant to the biological

implications of the data. Additionally, the constraint of the count total causes the abundance of different taxa to appear to be negatively correlated with each other when analyzed by conventional statistics. When one taxa increases in abundance, the counts detected in other taxa decrease in abundance, even if the taxa are not decreasing in abundance biologically. For example, one study compared the microbiome of vaginal swab samples from women with bacterial vaginosis (BV), women without BV, and women with intermediate BV, using qPCR to quantify the taxa. *Prevotella* was found to increase through non-BV to intermediate to BV, while *Lactobacillus iners* stayed relatively the same. If the same samples were put through a gene tag sequencing experiment where the taxa could not be quantified and the total read counts were constrained, one might incorrectly conclude that the abundance *Lactobacillus iners* was decreasing while *Prevotella* was increasing.

To prevent incorrect conclusions, data should be analyzed in a compositional way. In Euclidean space, data points can increase or decrease freely. Compositional data is under a sum constraint, and exist in a non-Euclidean space known as the Aitchison simplex [1]. A data transformation can be performed to put the data into Euclidean space, so that it can be analyzed with standard statistical methods that depend on Cartesian coordinates and linear relationships. These transformations involve examining the ratios of different OTU abundances to each other, so that the total number of reads do not unduly affect the result. In the example with bacterial vaginosis, using ratios of taxa to each other would elucidate the nature of the biological change in the data.

### 2.0.3 Unweighted UniFrac

Unweighted UniFrac [52] uses an inferred evolutionary distance to measure similarity between samples. It requires a reference phylogenetic tree containing all the taxa present in the samples to be examined, plus information about which taxa were detected in each sample. The calculation is performed by dividing the branch lengths that are not shared between the two samples by the branch lengths covered by either sample. Figure 2.1 shows example calcualtions for UniFrac based on the tree overlap. A distance of 0 means that the samples are identical, and a distance of 1 means that the two samples share no taxa in common.

As UniFrac is a binary test of absence, it is sensitive to sequencing depth, and assumes that the data has been normalized to a common sequencing depth [53], and rarefaction prior to unweighted UniFrac has become a standard part of the microbiome analysis workflow, with built in rarefaction functions in QIIME [11] and mothur [79].

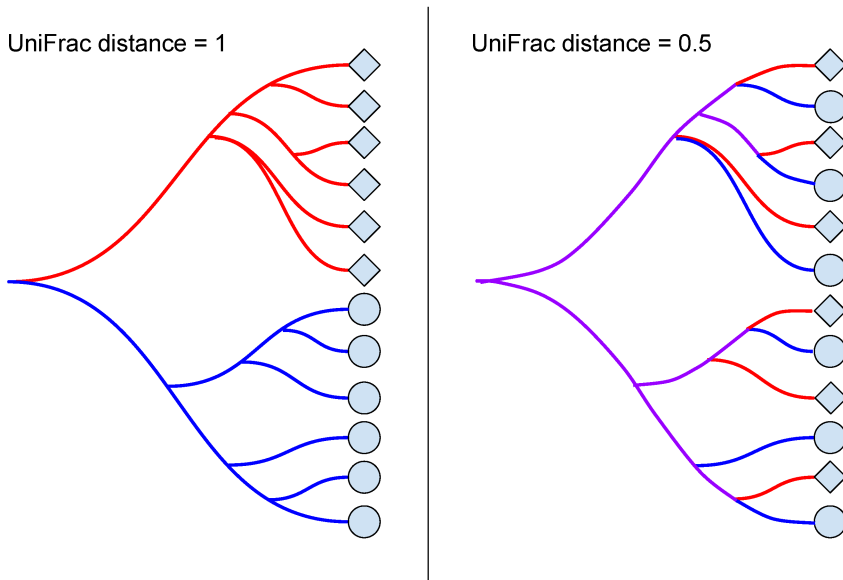


Figure 2.1: **Unweighted UniFrac.** When two samples do not share any branches of the phylogenetic tree, the unweighted UniFrac distance is maximized at 1. When two samples share half of their branch lengths on the phylogenetic tree, the unweighted UniFrac distance is 0.5. If the two samples contain exactly the same taxa, the unweighted UniFrac distance is minimized at 0, since the samples share all branches.

## 2.0.4 Weighted UniFrac

Weighted UniFrac [51] is an implementation of the Kantorovich–Rubinstein distance in mathematics, also known as the earth mover’s distance [25]. Rather than looking only at the presence or absence of taxa, each branch length of the phylogenetic tree is weighted by the difference in proportional abundance of the taxa between the two samples.

This technique reduces the problem of low abundance taxa being represented as a 0 or by a low count depending on sampling depth. In unweighted UniFrac, such taxa would flip from absent to present, and could skew the measurement: this would be especially problematic if the taxa are on a long branch. In weighted UniFrac, low abundance taxa have a much lower weight and so will have a lower impact on the total distance reported by the metric.

UniFrac is constituted as either a binary weighting (unweighted UniFrac) [52], a linear proportion (weighted UniFrac) [51], or some combination of the two (generalized UniFrac) [14]. However, it is a misconception that the data are linear because the sum of the total number of reads is constrained by the sequencing machinery [30] [26] [27] [50]. Microbiome communities can exhibit tremendous variation in their total bacterial count. For example, a stool sample may produce more highly concentrated DNA extract than a skin swab sample, resulting in different read count totals. Vaginal samples from patients with bacterial vaginosis compared to patients without can have total counts that differ one magnitude [103]. Alternative weightings

and non-linear transformations of data need to be explored. Furthermore, unweighted UniFrac is known to be unreliable, but it is not generally known or understood how this can impact results. 109  
110

## Materials and Methods 111

### 2.0.5 Analytical techniques 112

#### Rarefaction 113

Rarefaction normalizes the samples OTU counts to a standard sequencing depth [84]. This resulting table can be thought of as a random point estimate of the dataset, as the output is a sub-sample without replacement of the original table. This standardization process is recommended by the authors of UniFrac [13] in order to account for the sensitivity of UniFrac to sequencing depth. 114  
115  
116  
117  
118

Rarefactions can be performed using the QIIME software [11] or using the vegan package in R [63]. 119  
120

#### Unweighted UniFrac 121

Unweighted UniFrac is calculated based on the presence or absence of counts for each branch in the phylogenetic tree, when comparing two samples. A branch belongs to a sample when at least one of the OTUs in the leaves below it have a non-zero abundance. The formula for unweighted UniFrac is as follows, where  $b$  is the set of branch lengths in the phylogenetic tree,  $A$  and  $B$  represent the two samples being compared,  $\Delta$  is the symmetric difference between two sets, and  $\cup$  is the union between two sets: 122  
123  
124  
125  
126  
127

$$Unweighted_{AB} = \frac{\sum b_A \Delta b_B}{\sum b_A \cup b_B}$$

The sum of the branch lengths that belong to one sample but not the other is divided by the sum of the branch lengths that belong to one or both samples. 128  
129

#### Weighted UniFrac 130

Weighted UniFrac [51] also incorporates each branch length of the phylogenetic tree, and weights them according to proportional abundance of the two samples. The formula for weighted UniFrac is as follows, where  $A$  and  $B$  are the two samples,  $b$  is the set of branch lengths, and  $\frac{A_i}{A_T}$  and  $\frac{B_i}{B_T}$  are the proportional abundances associated with branch length  $b_i$ : 131  
132  
133  
134

$$Weighted_{AB} = \sum_i^n b_i \times \left| \frac{A_i}{A_T} - \frac{B_i}{B_T} \right|$$

#### Information UniFrac 135

Information UniFrac is calculated by weighing each branch length by the difference in the uncertainty of the taxa abundance between the two samples. Uncertainty information is calculated as follows, where  $p$  is the proportional abundance [83]: 136  
137  
138

$$\text{information} = -p \times \log_2(p) \quad (2.1)$$

If a sample is composed of 50% taxa A and 50% taxa B, then the proportional abundances have maximum uncertainty about what taxa is likely to be seen in a given sequence read. If a sample is 80% taxa A and 20% taxa B, then there is less uncertainty, because a given sequence read is more likely to be taxa A. When the amount of uncertainty that a taxa has in one sample corresponds with the amount of uncertainty the same taxa has in a different sample, the abundance of that taxa is mutually informative between samples. Weighting UniFrac by uncertainty combines the the concept of uncertainty with phylogenetic relationships to identify taxa that are differentially informative between groups.

The formula for Information UniFrac is as follows:

$$\text{Information}_{AB} = \sum_i^n b_i \times \left| \frac{A_i}{A_T} \log \left( \frac{A_i}{A_T} \right) - \frac{B_i}{B_T} \log \left( \frac{B_i}{B_T} \right) \right|$$

Information UniFrac approaches a minimum of zero (Fig. 2.5) when a sample is composed of a monoculture. It also related to the Aitchison distance in compositional data analysis [24].

### Ratio UniFrac

In complex microbiome communities, there may be a large number of bacterial taxa with few counts, such that the data is sparse. Taking the geometric mean of the proportional abundances of taxa in a microbiome sample represents an unbiased baseline of the average abundance of features with geometric growth characteristics - such as bacteria which divide by fission [1]. Experiments generally do not have power to detect differences at abundances below the mean [26]. Centering the proportional abundances around the geometric mean thus allows one to examine the data in this context, muting differences that are close to the baseline abundance and accentuating outliers. The formula for ratio UniFrac is as follows, where  $gm$  is the geometric mean:

$$\text{Ratio}_{AB} = \sum_i^n b_i \times \left| \frac{\frac{A_i}{A_T}}{gm(A_i)} - \frac{\frac{B_i}{B_T}}{gm(B_i)} \right|$$

Note that the geometric mean is calculated by combining all children in the subtree of  $b_i$  into  $\frac{A_i}{A_T}$  for sample A or  $\frac{B_i}{B_T}$  for sample B, and including the rest of the single taxa proportional abundances separately. The one combined proportional abundance and the remaining single taxa proportional abundances are input into the geometric mean formula, as set  $a$ :

$$gm(a) = \left( \prod_i^n a_i \right)^{1/n}$$

One challenge when it comes to the analysis of read count data is that the data is very sparse. Whether a low-abundance taxa or feature appears in the data as a zero or a low positive count

is up to chance, and assuming that a zero count represents the absence of a taxa can be very misleading [26]. A Bayesian approach can be used to give a posterior estimate of the likelihood for zero: this is implemented by the cmultRepl command in the zCompositions package in R [67].

The use of ratio weighting for UniFrac produces measurements that violate the metric triangle inequality, such that Euclidean statistics are technically invalid. Thus this metric, like the Bray-Curtis metric, is a dissimilarity, not a distance.

For this paper, we calculate UniFrac metrics using a custom R script, which includes unweighted UniFrac, weighted UniFrac, information UniFrac, and ratio UniFrac: [https://github.com/ruthgrace/ruth\\_unifrac\\_workshop](https://github.com/ruthgrace/ruth_unifrac_workshop)

### Bray-Curtis dissimilarity metric

The Bray Curtis dissimilarity metric [5] quantifies how dissimilar two sites are based on counts. A Bray-Curtis index of 0 means that two samples are identical, while a Bray-Curtis index of 1 means samples do not share any species. It is computed as a proportion through the formula:

$$C_{ij} = 1 - \frac{2C_{ij}}{S_i + S_j}$$

where  $C_{ij}$  = dissimilarity index bound by [0,1]

$S_i$  = Specimen counts at site i

$S_j$  = Specimen counts at site j

## 2.0.6 Data preparation

The data used comes in the form of a table of counts per operational taxonomic unit per sample, plus a phylogenetic tree. All of our data are derived from 16S rRNA gene tag sequencing experiments, and the data and scripts can be accessed at [https://github.com/JRWu/R\\_Scripts](https://github.com/JRWu/R_Scripts).

### Tongue dorsum data set

The tongue dorsum data set is a collection of 60 microbiome samples taken from the tongues of healthy participants. There were 0.3 million reads across 554 OTUs, and a minimum and maximum of 659 and 17176 reads per sample.

Samples from this experiment were sourced from the Human Microbiome Project [95] Qiime Community profiling v35 otu tables (<http://hmpdacc.org/HMQCP/>).

Rarefaction was conducted through Qiime version 1.8.0-20140103 to 659 reads (the lowest number of reads for a sample), and generation of the ellipse figures was done in R version 3.2.3 (2015-12-10) "Wooden Christmas-Tree" x86\_64-apple-darwin13.4.0 (64 bit).

A principal component analysis is drawn from each distance matrix per metric, and for the first principal component of each metric, the resultant value ( $V_{res}$ ) is computed per each first principal component as defined by the formula:

$$V_{res} = \frac{|V_1 - V_i|}{range(V_1, V_i)}$$

where  $V_{res}$  = Set of computed PC1s,

$V_1$  = Reference PC1 (the first),

$V_i$  = Each subsequent PC1,

### Tongue dorsum and buccal mucosa data set

The tongue dorsum and buccal mucosa data set is a collection of 30 microbiome samples taken from the tongues of healthy participants, plus 30 microbiome samples taken from the buccal mucosa (cheek) of a different set of healthy participants. There were 0.4 million reads across 12701 OTUs, and a minimum and maximum of 5028 and 9861 reads per sample. Note that if the OTUs that are less than 1% abundant in all samples are filtered out, only 179 OTUs remain.

To create this data set, thirty random samples were selected from the tongue site of the Human Microbiome Project [95] and thirty random samples from the buccal mucosa site. Samples were filtered so that only samples with 5000 to 10,000 reads were included.

Read counts from the HMP data set were rarefied to the smallest total read count per sample using the vegan R package [63] before the unweighted UniFrac distance was calculated. Weighted, information, and ratio UniFrac were calculated on the data set without rarefaction. The resulting distances were plotted for principal component analysis.

### Breast milk data set

The breast milk data set is a collection of 58 microbiome samples taken from lactating Caucasian Canadian women. The breast milk data set used here has also been published in a recent study [96]. There were a total of 5.3 million reads across 115 OTUs, and a minimum and maximum of 3072 and 2.8 million reads per sample. Note that the 2.8 million reads came from a sample that was taken from a patient with an infection, and the next largest number of reads per sample was 282485 (ten times less).

The count table was analyzed using our custom UniFrac script, which can be accessed at [https://github.com/ruthgrace/ruth\\_unifrac\\_workshop](https://github.com/ruthgrace/ruth_unifrac_workshop). Data was rarefied to the sample with the smallest number of read counts (3072) before the unweighted UniFrac distance matrix was calculated. Non-rarefied data was used for weighted, information, and ratio UniFrac. Data was plotted using a principal components or coordinate analysis as appropriate.

### Monoculture data set

The monoculture data set is simulated based on the infected sample from the breast milk data set. Each simulated sample has exactly the same counts per taxa as the infected sample, except that the taxa are shuffled. After taxa shuffling, the data was manipulated into two groups. In one set of 20 samples the taxa with the highest count was swapped with *Pasteurella*, in another set of 20 the taxa with the highest count was swapped with *Staphylococcus*, and in the last set of 20 the taxa with the highest count was swapped with *Pseudomonas*. These three taxa were

picked because they were the most highly abundant in the original breast milk data set. This process produced three sets of monocultures, dominated by the three different taxa. 229  
230

## Results 231

### 2.0.7 Unweighted UniFrac is highly sensitive to rarefaction instance 232

A commentary by Lozupone et al. 2011 [53] addressed the sensitivity of Unweighted UniFrac to sampling. Lozupone's group used mean UniFrac values to compute a confidence ellipse between the first and third quartile. However, we observed that this approach under-represented the true variability of unweighted UniFrac as a distance metric by highlighting how individual samples vary. In the absence of true differences and in the presence of uneven sampling, unweighted UniFrac can be sensitive to rarefaction instances. We show this by analyzing two rarefactions of the same body site with the rationale that if there is no true difference in the data, separation of these samples should not be observed. 233  
234  
235  
236  
237  
238  
239  
240

Sixty tongue dorsum subsamples were drawn from the Human Microbiome Project data without replacement. Rare OTUs with less than 100 total counts across all the samples were removed. The minimum sample count for the subset of 60 we analyzed was 659, therefore we rarefied (subsampled) to the minimum of 659 to normalize the samples, prior to performing a principal coordinates analysis (PCoA). For Fig. 2.2, two independent rarefactions of the data were conducted in order to observe the effect of rarefaction instance on the metric. The unweighted UniFrac distance was computed for each rarefaction, and Procrustes adjustment was applied in order to overlay the PCoA-derived second rarefaction onto the first. A PCoA of rarefaction 1 was plotted, and any samples that changed between rarefactions one and two were visualized with red and blue on the plot. If the sample moved from one side of the first component axis to the other between the rarefaction instances, it was indicated with either a blue or a red arrow. 241  
242  
243  
244  
245  
246  
247  
248  
249  
250  
251  
252

In both rarefactions on Fig. 2.2, samples separated distinctly into two clusters on principal component 1. Principal component 1 explains the most variation in the data, and is thus useful to visualize if any associated metadata is behind the sample separation. However, the separation was not explainable by any metadata associated with the HMP experiment, and is thus an undesirable result. When plotting the rarefactions against each other, several samples are observed to be unstable, exhibiting large differences in location. This example demonstrates that samples with little difference can appear to be different through the unweighted UniFrac distance metric and that rarefaction can lead to misleading and non-reproducible results. 253  
254  
255  
256  
257  
258  
259  
260

For the ellipse plot in Fig. 2.3, 60 tongue dorsum subsamples were randomly drawn without replacement. Rare OTUs with less than 100 total counts across all samples were removed. A hundred separate rarefactions were conducted on the data to a minimum sampling depth of 378. For each individual rarefied OTU table, a distance matrix was computed using one of unweighted UniFrac, weighted UniFrac, Bray-Curtis Dissimilarity, information UniFrac, or ratio UniFrac as the weighting method. By generating 100 separate datasets for each metric, it is possible to assess the effect of rarefaction instance on each metric by analyzing what is essentially the same data. In other words, what does the effect of random sampling (rarefaction) have on the output of each metric? Each distance matrix generated per metric was adjusted with 261  
262  
263  
264  
265  
266  
267  
268  
269

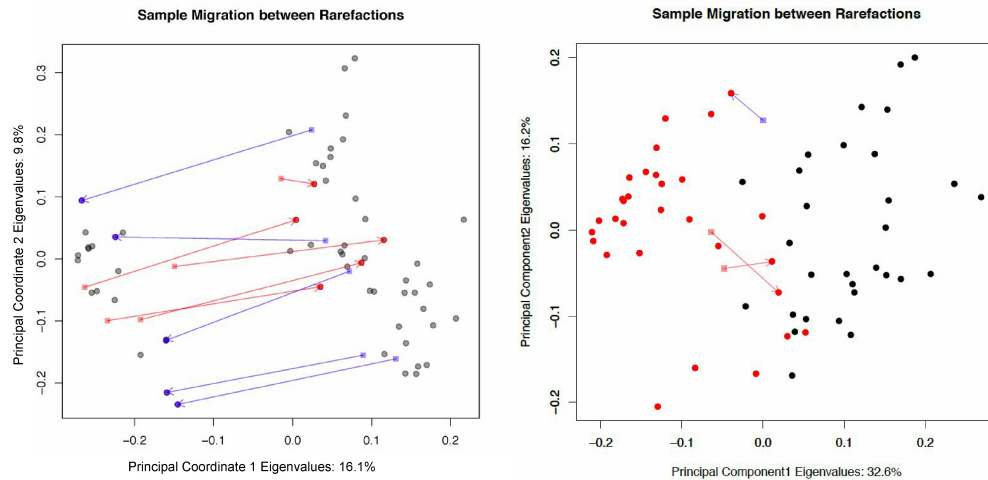


**Figure 2.2: Sample migration in different rarefactions, plotted on principal components, measured with unweighted UniFrac.** The left plot is of the tongue data set while the right plot is the tongue dorsum vs. buccal mucosa data set. On the left panel red samples have moved from the left cluster to the right cluster between rarefactions. Blue samples have moved from the right cluster to the left. Samples are taken from the tongue dorsum body site from the Human Microbiome Project database. If the experiment were run once, one might mistakenly assume that there are two clusters of data, however, the inconsistent sample membership of the two groups between rarefactions proves the clustering irreproducible. The tongue dorsum and buccal mucosa data set is included for comparison, with the tongue samples colored black and the buccal mucosa samples colored red. Note that the variance explained in the tongue data set by the first and second component is merely 16.1% and 9.8% respectively, indicating that the data is rather spherical, even though the points on the plot appear to show two separated clusters (compare with 32.6% and 16.2% in the tongue dorsum vs. buccal mucosa data set). The variance explained in the first and second component in the 2011 UniFrac commentary [53] was even smaller, at 8.6% and 5.6%.

a Procrustes adjustment to overlay the subsequent rarefactions onto the first.

The maximum value of Vres for each rarefaction is plotted against the median value per rarefaction in Fig. 2.3. This plotting serves to highlight the maximum potential change for an analysis given that there is no difference in the data. Unweighted UniFrac shows by far the highest maximum potential change between rarefactions, compared to weighted, information, and ratio UniFrac, as well as Bray-Curtis.

Given the wide use of unweighted UniFrac in the literature with small principal component 1 and 2 effects, we suggest caution in their interpretation. For example, see the use of unweighted UniFrac in these papers about the human microbiome published in Cell[38], where the first and second principal components axis explain 14% and 9.5% of the variation in Figure 2A, as well as in Nature [87], where the first principal component explains 14% of the variation in Figure 1. In both of these examples, less variance is explained by the first principal component than in our uniform tongue data set.

270

271

272

273

274

275

276

277

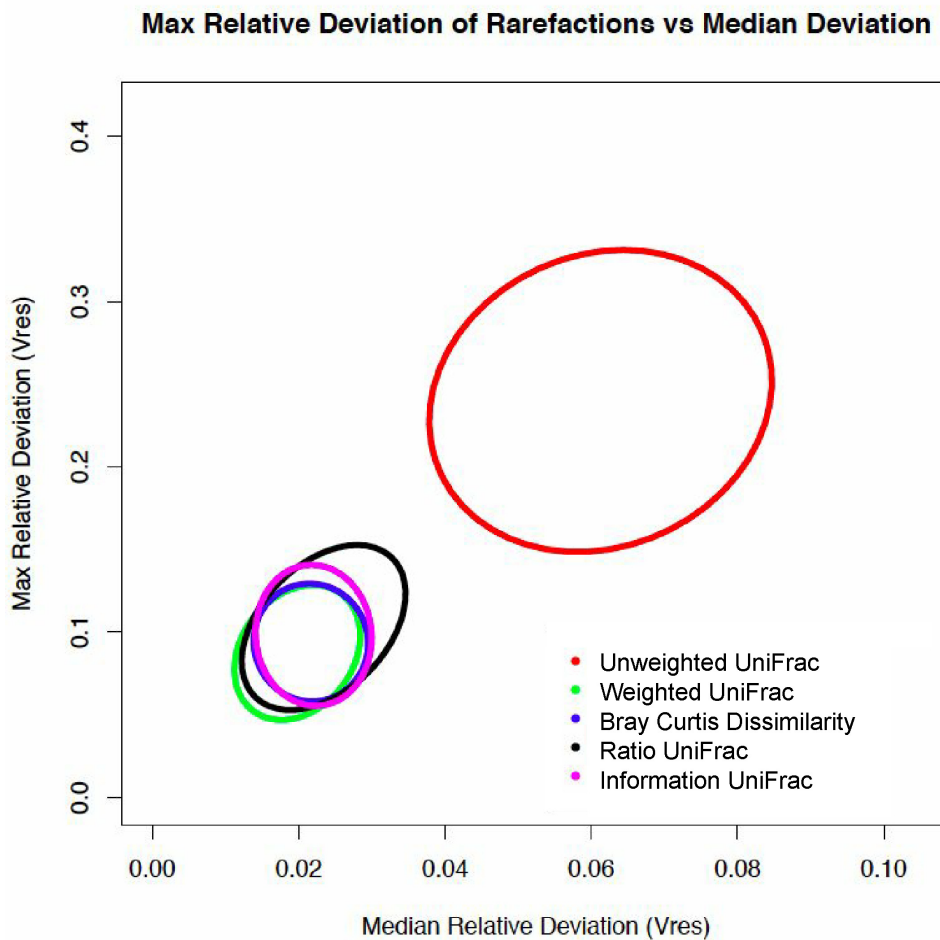
278

279

280

281

282

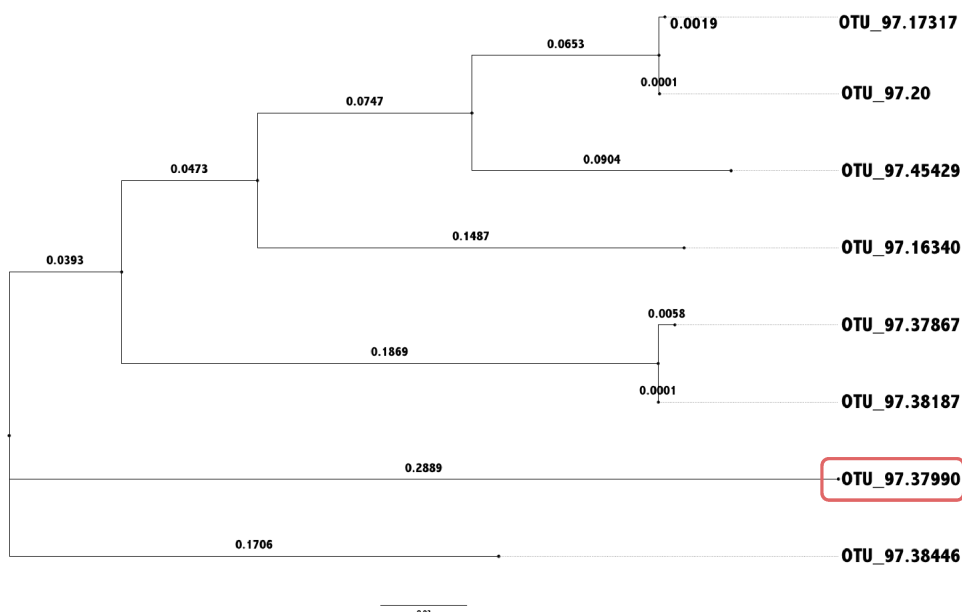


**Figure 2.3: Maximum relative deviation of rarefactions versus median deviation for traditional and non-traditional microbiome dissimilarity metrics.** Sixty samples from the tongue dorsum were taken from the Human Microbiome Project [95], and rarefied 100 times. The maximum relative deviation was plotted against the median relative deviation of the rarefied data, and ellipses were drawn at the 95% confidence interval, around the cloud of points for each metric. A higher maximum and median deviation indicates lower reproducibility of results between rarefaction instances. Both the maximum relative deviation of rarefied data and the median relative deviation of rarefied data are greater in unweighted UniFrac than in weighted UniFrac, Bray Curtis distance, ratio UniFrac, and information UniFrac.

## 2.0.8 The cause of rarefaction variation by Unweighted UniFrac

283

One point to note is that rarefaction carries the assumption that microbiota within samples are homogeneous and randomly distributed. However, this assumption is only valid if proper sampling protocols are observed [34]. A combination of unevenly sampled OTUs and distantly related OTUs will contribute to the variability in unweighted UniFrac when OTUs are ultimately rarefied. Distance matrices between samples will be affected when rare OTUs are left out during the rarefaction processes. It becomes intuitive to see how similar samples may grow dissimilar from each other through unweighted UniFrac on rarefied samples as the number of unshared branches increases as OTUs are removed.

284  
285  
286  
287  
288  
289  
290  
291

**Figure 2.4: Phylogenetic tree with long isolated branches.** Variation in different rarefactions of data in unweighted UniFrac analysis is exacerbated by the presence of long isolated branches in the phylogenetic tree, such as the circled OTU in this example.

292  
293  
294  
295  
296

With rare OTUs and long branch lengths in the phylogenetic tree (Fig. 2.4), the Unweighted UniFrac distance metric on rarefied data is highly variable, declaring the samples A and B identical (distance of 0) with 1 rarefaction, and different with another (distance of 0.4175), as demonstrated in Table 2.1 and the calculations above.

297  
298  
299  
300  
301  
302  
303  
304

While an improvement on unweighted UniFrac, weighted UniFrac can overweight differences between large proportional abundances and underweight differences between small proportional abundances. If one bacterial taxa increased in proportion from 5/1000 to 10/1000 and another taxa increased in proportion from 95/1000 to 100/1000, they would have the same weight in weighted UniFrac. However, the first taxa has doubled in proportion between samples, and this is much more biologically significant than the change in proportional abundance in the second taxa. Additionally, it does not account for how the counts add up to a constrained sum determined by the sequencing machine model. Because the sum is constrained, as with the

Table 2.1: **Original abundance of taxa and rarefied abundance of taxa.** This data was simulated to demonstrate how rarefaction can change the distances reported by the unweighted UniFrac metric. The OTU in bold has been rarified to a zero count in sample A for one instance and a non zero count in the other instance. In Rarefaction 1, the unweighted UniFrac distance (unshared over total branches) is 0.4175, while in Rarefaction 2 the distance is 1.12.

OTU.ID	A	B	A R1	B R1	A R2	B R2
OTU.16340	52	1	8	1	12	1
OTU.17317	17	4	3	4	5	4
OTU.20	70	18	14	18	20	18
OTU.37867	59	10	9	10	11	10
<b>OTU.37990</b>	7	59	<b>0</b>	59	<b>1</b>	59
OTU.38187	646	115	132	115	122	115
OTU.38446	6	8	0	8	1	8
OTU.45429	218	6	55	6	49	6

bacterial vaginosis sample earlier, an increase in growth of one taxa can make the data look like there is a decrease in abundance in other taxa, even if in reality the population of the other taxa stayed the same.

Here we explore some alternatives to unweighted and weighted UniFrac, and discuss their merits and shortfalls.

## 2.0.9 Information UniFrac

The difference in information content between taxa with low proportional abundances (which make up the bulk of microbiome data) is generally higher than the difference between the proportional abundances themselves, potentially allowing scientists to differentiate samples with subtle differences, such as the infected breastmilk sample in Fig. 2.7.

For example, Fig. 2.5 shows the weighting of a taxon in unweighted, weighted, and information UniFrac as a function of the taxon proportional abundance. Near the 0, 0 point the proportional abundances are low and information is 0. However, small increases in abundance result in large changes in contribution to UniFrac weighting, as shown by the slope of the curve. Here there is higher differentiation between weights of different pairs of low proportional abundances for information UniFrac, as shown by the higher slope of the curved graph. The ratio UniFrac (not depicted) depends on the geometric mean of the taxonomic abundances, and each sample would have a different slope in the weight graph depending on how evenly the abundances were distributed.

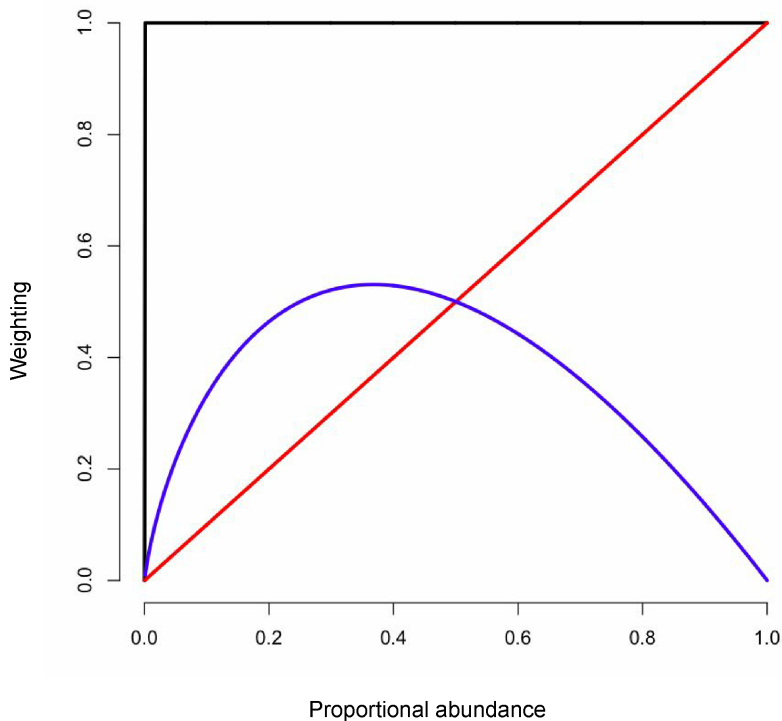


Figure 2.5: **UniFrac weights.** Each UniFrac weighting is plotted with the corresponding proportional abundance. The black line is unweighted UniFrac, the red line is weighted UniFrac, and the blue line is information UniFrac. From 0 to 0.2 on the x-axis information UniFrac has a higher slope, and therefore more discovery power with smaller changes in abundance. As the x-axis approaches 1, changes in abundance add little discovery power to information UniFrac.

### 2.0.10 Tongue and buccal mucosa comparison

We next explore two other datasets, one with a defined difference between groups (tongue dorsum compared to buccal mucosa), and one with an outlier that is only apparent when analyzed by certain dissimilarity metrics.

Fig. 2.6 shows a principal component analysis plot with four different metrics: unweighted UniFrac, weighted UniFrac, information UniFrac, and ratio UniFrac. We observe that the difference in the microbiome between the human tongue and buccal mucosa are well defined by all metrics (Fig. 2.6), since all of the weightings show separation between the samples according to body site. We conclude from (Fig. 2.3) that weighted UniFrac, information UniFrac, and ratio UniFrac do not tend to show spurious separation in uniform data sets to the degree that unweighted UniFrac does, while reliably separating samples in data with a defined difference between groups.

324  
325  
326  
327  
328  
329  
330  
331  
332  
333  
334  
335

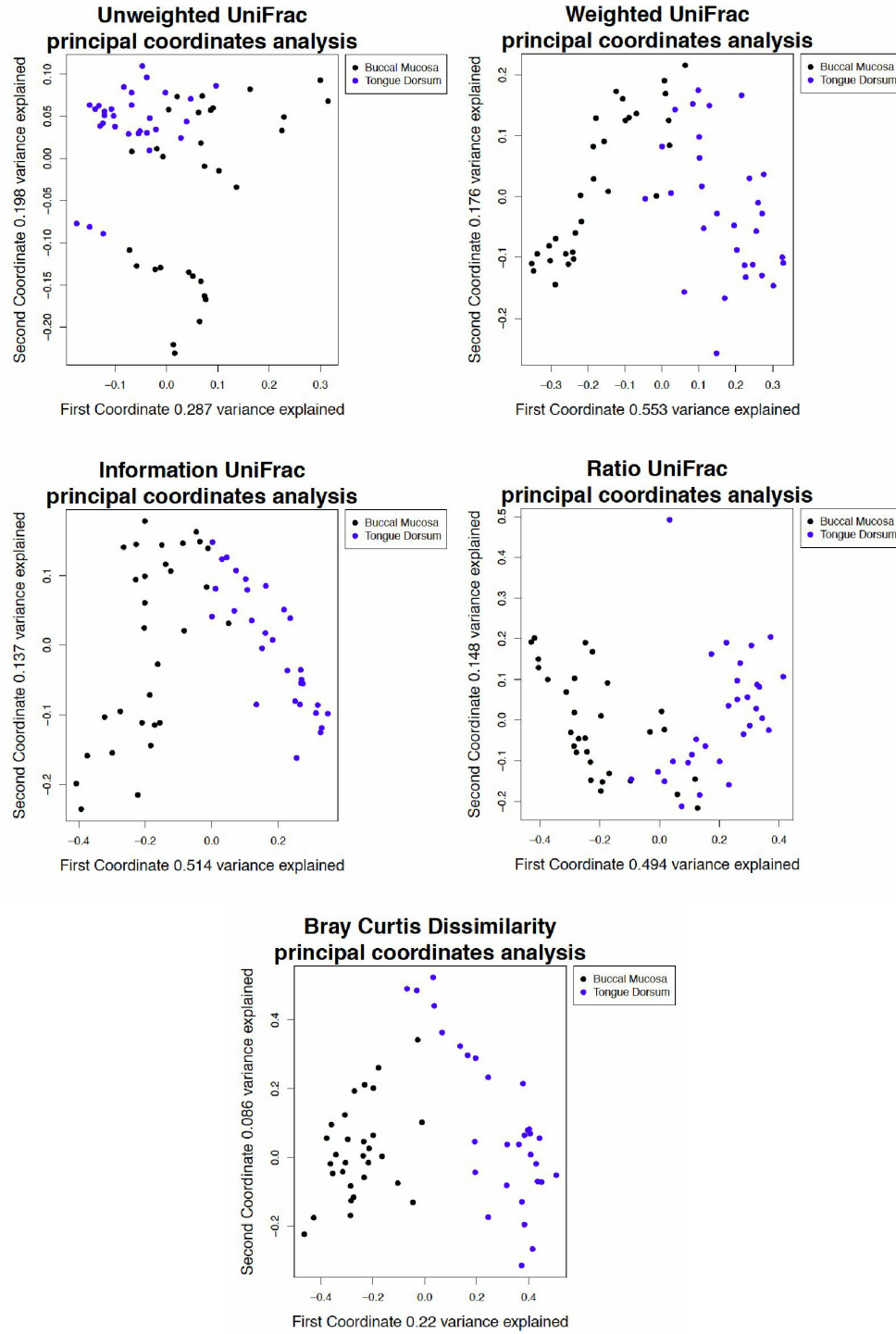


**Figure 2.6: Analysis of tongue and buccal mucosa data using different UniFrac weightings.** A principal component analysis of a 16S rRNA gene tag experiment done on samples from the tongue and buccal mucosa, selected from the Human Microbiome Project [95]. All weightings and the Bray-Curtis dissimilarity show separation between the samples by body site. Note that the variance explained by the first and second principal component axis is higher than in the tongue-tongue data set from Figure 2, which had 16.1% and 9.8% variance explained, respectively.

## 2.0.11 Breast milk Data

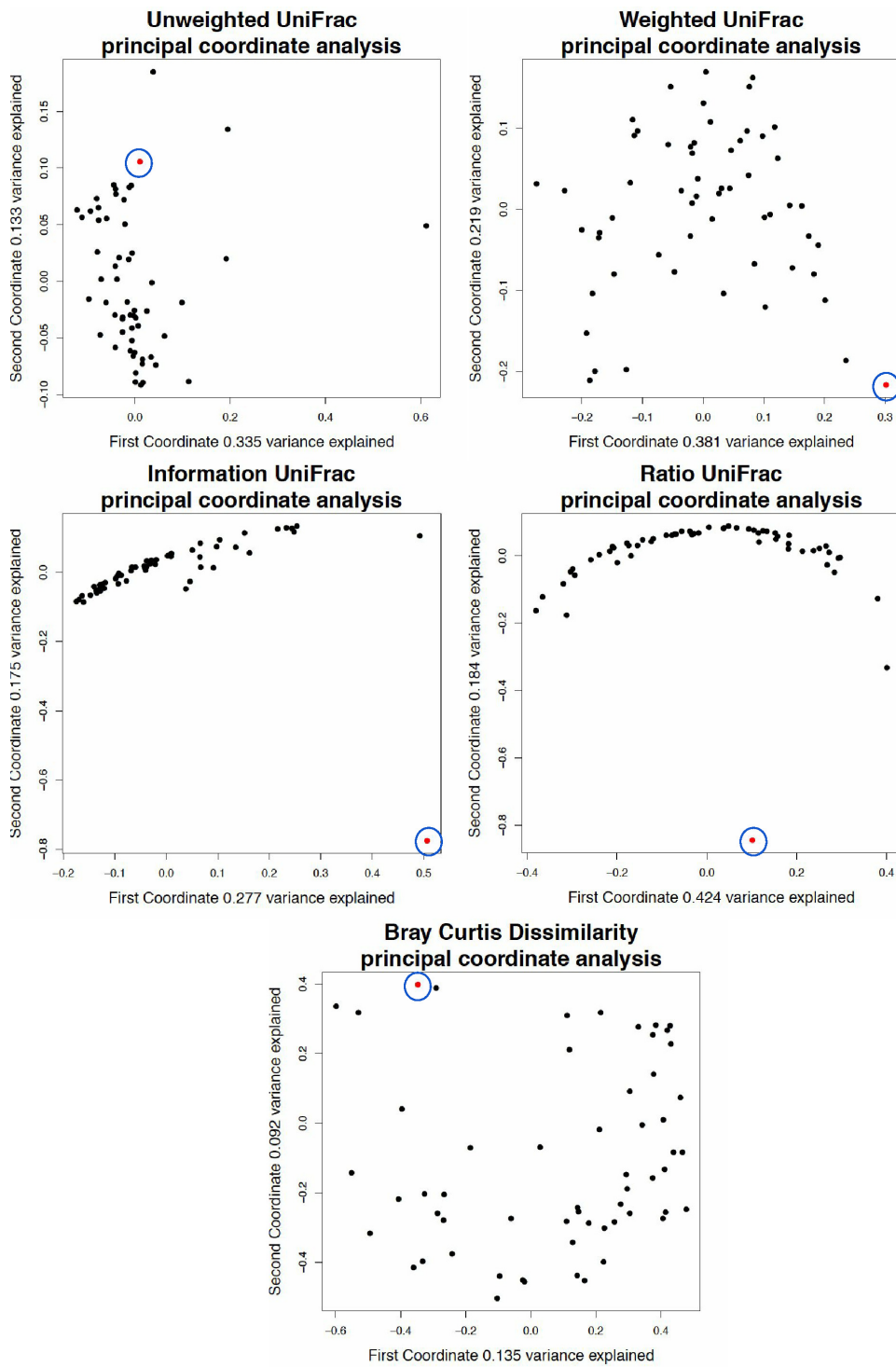
336

Fig. 2.7 is a principal component analysis of a 16S rRNA gene sequencing experiment done  
337 on microbiome samples from breast milk [96]. Breast milk samples were collected and the V4  
338 region of the 16S rRNA gene was sequenced. One of the patients who provided a sample had  
339 an active infection, producing a sample that consisted of 97% Pasteurella. We noted that this  
340 sample was not distinct in unweighted and weighted UniFrac because the distance from the  
341 Pasteurella branches of the phylogenetic tree to the root of the tree (rooted by midpoint) were  
342 not particularly short or long, measuring at just over the 3rd quartile of all root-to-leaf distances.  
343 In addition, the Pasteurella leaves shared a clade with many other taxa.  
344

345

The reason the infected sample in the breast milk study is so distinct from the rest of  
346 the samples in Information UniFrac and Ratio UniFrac is because of the weighting. The  
347 infected sample was 97% Pasteurella, while the other samples generally had 15-20% each of  
348 Staphylococcus and Pseudomonas, and little or no Pasteurella. Unweighted UniFrac does not  
349 differentiate between high and low abundance. Weighted UniFrac does, placing the infected  
350 sample in the bottom right corner of that plot. Information UniFrac weights everything in the  
351 infected sample close to zero, as taxa are present in either very high or very low abundance,  
352 while weighting Staphylococcus and Pseudomonas in the other samples highly (around 0.4) due  
353 to their 15-20% abundance. Ratio UniFrac recognizes that the infected sample has a taxonomic  
354 abundance very far from the geometric mean abundance. For these reasons information and  
355 ratio UniFrac are more adept at picking up outliers with uneven distributions, even if the taxa  
356 are shared by other samples.

356



**Figure 2.7: Analysis of simulated monocultures using different UniFrac weightings.** A principal component analysis of a simulated 16S rRNA gene tag experiment based on the breast milk data. Red samples are dominated at 07% by *Pasteurella*, black samples are dominated by *Staphylococcus*, and cyan samples are dominated by *Pseudomonas*. Note that while information UniFrac appears to separate the samples reasonably well visually, the amount of variance explained by the first two components is much lower than even weighted UniFrac.

## 2.0.12 Monoculture data

357

Each sample in the monoculture dataset is 97% dominated by one of three taxa. However,  
358  
within the remaining 3% there is variation in the counts.  
359

360

Unweighted UniFrac, being binary test, detects only the variation in the remaining 3% of  
360 counts, without showing the difference in the monocultures. Weighted UniFrac detects only  
361 the difference in the identity of the monoculture, and the separation is driven by phylogenetic  
362 distance - the pairwise distance from *Pasteurella* to *Staphylococcus* and *Pseudomonas* to  
363 *Staphylococcus* is just over 0.9 on the phylogenetic tree while the distance from *Pasteurella* to  
364 *Pseudomonas* is 0.45. This is in correspondence with the PCoA plot where the first component  
365 (which separates the *Staphylococcus* species from the other two) explains over 90% of the  
366 variance in the data set.  
367

368

Information UniFrac is known to not perform very well for monocultures, due to taxa with  
368 very high and low proportional abundances having uncertainty information values close to  
369 zero (Fig. 2.5). While the samples separate visually with information UniFrac, the variance  
370 explained by the separation is low, and the distance matrix does not separate the three groups by  
371 hierarchical clustering. Ratio UniFrac and Bray Curtis both separate the samples by monoculture,  
372 and also differentiate the samples by their minor variations, showcasing a more representative  
373 perspective of this data set.  
374

375

If the samples are hierarchically clustered, the three groups separate perfectly with weighted  
375 UniFrac, ratio UniFrac, and Bray Curtis dissimilarity, but not with unweighted UniFrac or  
376 information UniFrac.  
377

378

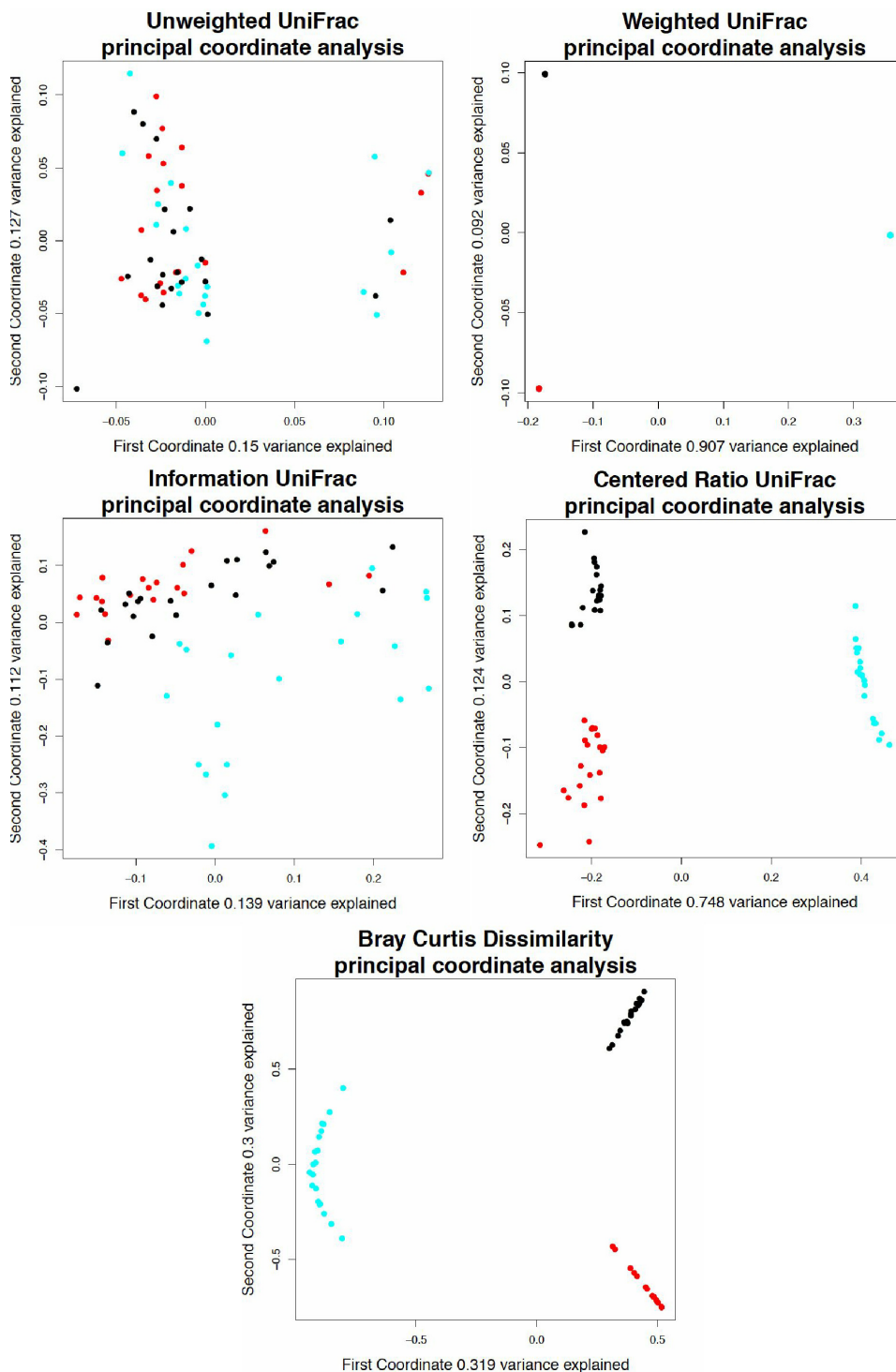


**Figure 2.8: Analysis of simulated monocultures using different UniFrac weightings.** A principal component analysis of a simulated 16S rRNA gene tag experiment based on the breast milk data. Red samples are dominated at 97% by *Pasteurella*, black samples are dominated by *Pseudomonas*, and cyan samples are dominated by *Staphylococcus*. Note that while information UniFrac appears to separate the samples reasonably well visually, the amount of variance explained by the first two components is much lower than even weighted UniFrac.

## Discussion

378

As shown in the tongue and buccal mucosa data set, unweighted UniFrac is perfectly sufficient  
 379  
 for data sets with a notable difference. However, in data sets with no difference or a very small  
 380  
 difference between groups such the uniform tongue dorsum data set, unweighted UniFrac is the  
 381  
 least reliable and we found that it may produce wildly different results depending on rarefaction  
 382  
 and sequencing depth. This can result in spurious groups, or inclusion of samples in the wrong  
 383  
 groups.  
 384

We found weighted UniFrac, information UniFrac, ratio UniFrac, and Bray-Curtis methods  
 385  
 to be more reliable choices. We suggest that investigators use several methods as they can detect  
 386  
 outliers in different circumstances. When an outlier is detected by any metric, an investigation  
 387  
 is warranted, as with our example in the breast milk data set.  
 388

We do not believe that any of these weightings are a perfect model for microbiome data.  
 389  
 Each tool is prone to its own set of weaknesses. If the difference in groups is driven by  
 390  
 presence/absence then UniFrac is a reasonable choice. If the difference is driven by a linear  
 391  
 abundance, then weighted UniFrac is a good choice. Information UniFrac and ratio UniFrac  
 392  
 are useful for examining data sets that contain the similar sets of taxa between groups. Ratio  
 393  
 UniFrac is especially good for examining data sets that have more subtle variations, due to  
 394  
 its non linear nature. In any case, inspection should be done to make sure that the tool used  
 395  
 accurately represents the data.  
 396

In summary, with the addition of information UniFrac and ratio UniFrac, biologists have  
 397  
 more tools at their disposal to prevent spurious interpretations, detect outliers, and ultimately  
 398  
 understand their data better.  
 399

## Acknowledgments

400

Thanks to Camilla Urbaniak for providing the data from her breast milk study [96].  
 401

unifrac

# **Chapter 3**

## **The human microbiome and non-alcoholic fatty liver disease**

### **3.1 Introduction**

Non alcoholic fatty liver disease (NAFLD) has been on the rise along with obesity, affecting a fifth to a third of the North American population [72]. Most people with NAFLD remain asymptomatic, however, in up to a third of patients NAFLD can progress to non-alcoholic steatohepatitis (NASH), causing inflammation and scarring (fibrosis) in the liver, and decreasing the 5 year survival rate to 67% [73]. It is thus important to shed some light on the process by which people progress from NAFLD to NASH to find interventions that prevent NASH.

#### **3.1.1 NASH progression risk**

There are several known genetic and chemical factors that increase the risk of progression to NASH in animal models and humans.

##### **Mouse**

In mice non alcoholic fatty liver disease is often modelled with a methionine/choline-deficient diet (MCD), which induces steatohepatitis in wildtype mice. Mice with a toll-like receptor 4 knockout had lower lipid and injury accumulation markers when fed a MCD diet [77].

##### **Rat**

In rats liver fibrosis can be induced by drugs. One study found that male rats were more prone to this induced liver fibrosis than female rats. Fibrosis biomarkers were reduced when the male rats were dosed with estradiol, and increased when the male rats were additionally given an estradiol-neutralizing antibody. Female rats who had their ovaries removed similarly lost the protective effect [100]. From this, hormones are also a factor in non-alcoholic fatty liver disease progression.

##### **Human**

In humans, the I148M variant of the Patatin-Like Phospholipase Domain Containing 3 gene

(PNPLA3) correlates with a 3.2 fold increased risk of progression to NASH from NAFLD when homozygous, compared to patients without the variant [88]. The heterozygous gene was found to be associated with fatty liver disease in genome wide association studies, but some additional studies have failed to replicate the relationship with NASH [88].

On the epigenetic level, many genes are differentially methylated in advanced NAFLD compared to mild NAFLD. 11% of genes are differentially hypomethylated in advanced NAFLD (compared to 3% hypermethylated), leading to increased expression [61]. In advanced NASH specifically, some tissue repair genes were hypomethylated while some metabolism pathways such as 1-carbon metabolism were hypermethylated. However, only 7% of the differentially methylated genes were found to be differentially transcribed [61].

On a metabolite level, Raman et al. found differences in the number of volatile organic compounds detected in patients with NAFLD compared to obese patients without NAFLD [75]. Reactive oxygen species have also been implicated in NASH due to their involvement in the mechanism of steatohepatitis-inducing drugs [7].

The microbiome is thought to have an effect on host digestion and absorption of nutrients [32]. Fermenters produce short chain fatty acids, which make up 10% of the calories in a Western diet [59] Some groups claim a link between ethanol-producing gut bacteria and NAFLD [102] [40], however the evidence was inconclusive since no multiple test correction was performed.

### 3.1.2 Data

Applying next generation sequencing techniques to microbiome research is a relatively new field that has yet to set data analysis standards. There are some considerations that should be made when constructing a data analysis strategy.

#### Data is multivariate

Generally experiments of this nature typically have low sample sizes due to budget constraints, sample collection difficulties, patient compliance, and other issues.

As a result, the number of taxa or gene functions comparisons made are often a magnitude larger than the sample size. This is known in statistics as having more variables than observations, or having fat data. The higher the ratio of variables to observations are, the less likely standard statistical techniques are to be reliable [64].

Researchers should include multiple test corrections to ensure that the results they are reporting are true, at the expense of having p-values less than 0.05. Unfortunately many studies have been published in high impact journals without multiple test corrections, including a famous paper linking the gut microbiome to autism published in Cell [38].

#### Data is compositional

In both gene tag sequencing and metagenomic sequencing experiments, the data is in the form of a list of counts per feature, with the features composing an aspect of the microbiome for each sample. This is compositional data. The total number of reads yielded by the sequencing platform is often platform-dependant and not biologically relevant.

This constrained sum causes the abundance of different taxa to appear to be negatively correlated with each other when analyzed by conventional statistics. When one taxa increases

in abundance, the counts detected in other taxa decrease in abundance, even if the taxa are not decreasing in abundance biologically.

Compositional data should be analyzed in a compositional way. In Euclidean space, data points can increase or decrease freely. Compositional data is under a sum constraint, and exist in a non-Euclidean space known as the Aitchison simplex [1]. Data transformations such as the centered log ratio can be performed to put the data into Euclidean space, so that it can be analyzed with standard statistical methods that depend on Cartesian coordinates and linear relationships.

However, these techniques are not yet mainstream in the field, resulting in a high number of conclusions made that are not reproducible.

### 3.1.3 Literature

Several papers have already been published in the literature on the topic of NAFLD and the gut microbiome:

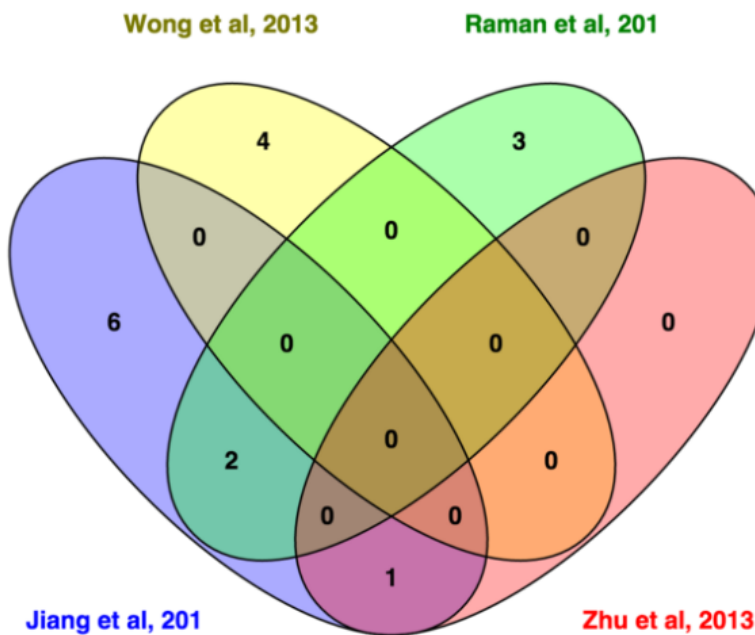


**Figure 3.1: Venn diagram of genera found to be differentially abundant by different studies between NASH/NAFLD and healthy controls.** Only 3 out of the 16 genera claimed to be differentially abundant were found in two studies: members of the *Escherichia* genus were found in the Zhu [102] and Jiang [40] studies, and members of the *Lactobacillus* and *Oscillibacter* genus were found in the Jiang [40] and Raman [75] studies.

#### Jiang et al, 2015 [40]

**Study:** This group compared 53 NAFLD patients with 32 healthy controls. The NAFLD patients had a significantly higher BMI ( $P < 0.01$ ).

**Sequencing:** Each sample had an average of 0.6 million reads, from sequencing the V3 region of the 16S rRNA gene on the Illumina sequencing platform.

**Analysis:** The reads were annotated with the Ribosomal Database Project [16] and differential abundance was determined using Projection on Latent Structures - Discriminant Analysis (PLS-DA) methods.

**Results:** They found a relative increase in members of the *Lentisphaerae* phyla and the *Oscillibacter* and *Flavonifractor* genera in the healthy group, and a relative increase in members of the *Clostridium XI*, *Anaerobacter*-related, *Streptococcus*, and *Lactobacillus* genera in the NAFLD group.

### Zhu et al, 2013 [102]

**Study:** This group compared 16 non-obese controls, 25 obese patients, and 22 NASH patients. All of the patients were pediatric, and the NAFLD group all had a BMI higher than the 85th percentile while the healthy group had BMIs less than the 85th percentile.

**Sequencing:** A 16S rRNA gene tag sequencing experiment was performed and reads were sequenced in a 454 pyrosequencer.

**Analysis:** This group used MG-RAST [60] and QIIME [11].

**Results:** Note that in the PCoA plot, there is only 11% variance explained by the first component, and they had to plot the first component with the 3rd component (3% variance explained) to show the group separation. By comparing the average absolute read count for each taxa in each group, this group found that members of the *Proteobacteria* phylum, the *Enterobacteriaceae* family, and the *Escherichia* genus had significantly higher average counts in NASH patients compared to obese patients and healthy controls.

### Raman et al, 2013 [75]

**Study:** This group compared 30 NAFLD patients with 30 healthy controls. All the healthy controls had a BMI less than 25 while all the NAFLD patients had a BMI greater than 30.

**Sequencing:** The 16S rRNA gene was amplified and sequenced with 454 pyrosequencing, yielding 2000 reads per sample.

**Analysis:** Reads were annotated with the Ribosomal Database Project [16]. UniFrac analysis was performed with QIIME [11], and differential abundance was tested with Metastats [68].

**Results:** They found a relative increase in members of the *Lactobacillus*, *Robinsoniella*, *Roseburia*, and *Dorea* genus in NASH patients and a relative increase in members of the *Oscillibacter* in healthy patients.

### Wong et al, 2013 [99]

**Study:** This group compared 16 NASH patients with 22 healthy controls.

**Sequencing:** They amplified the V1-V2 variable region of the 16S rRNA gene with pyrosequencing, yielding 4-11 thousand reads per sample.

**Analysis:** Reads were clustered with UCLUST [23] and annotated with the Ribosomal Database Project [16].

**Results:** Members of the the genera *Parabacteroides* and *Allisonella* were found to be relatively increased in NASH patients, while members of the genera *Faecalibacterium* and *Anaeropsporobacter* were relatively increased in healthy controls.

### Boursier et al, 2015 [8]

**Study:** This group compared 30 patients with F0 or F1 fibrosis to 27 patients with F2 or greater fibrosis, 35 of which had NASH

**Sequencing:** A gene tag experiment was performed on the V4 region of the 16S rRNA gene, and sequenced on an Illumina platform, yeilding an average of 0.2 million reads per sample.

**Analysis:** Reads were annotated with the Greengenes database [19], and differential abundance was measured by Mann-Whitney's test. A metagenomic imputation was performed with PiCrust [45], annotated with KEGG [41], and analysed with LEfSE [80].

**Results:** A relative increase in members of the *Bacteroides* phylum and a relative decrease in members of the *Prevotella* phylum was found in NASH, compared to healthy controls. From the metagenomic imputation, the gut microbiome of NASH patients was found to be significantly enriched functional categories related to carbohydrate, lipid, amino acid, and secondary metabolism.

Many of the studies had healthy controls with a lower BMI, so it is difficult to separate whether the differences found are related to NAFLD progression or obesity.

Fig. 3.1.3 shows a Venn diagram illustrating the inconsistency of the literature on the gut microbiome and NAFLD. Of these, only Raman et al [75] reported using a multiple test correction.

Since these five studies do not form a consistent story about the gut microbiome and NAFLD, we conducted own analysis rigorously, such that our results are replicable. Additionally, we generate the first deeply sequenced metagenomic sample set to examine functional capabilities in this disease.

## 3.2 Methods

In total, 67 samples were collected: 29 from patients with non-alcoholic steatohepatitis (NASH), 14 from patients with simple steatosis (SS), and 24 from healthy controls. The median BMIs were 26.70, 27.34, and 32.06, and the median ages were 36, 49, and 46.5 for healthy, SS, and NASH respectively.

DNA extraction was performed with the E.Z.N.A.® Stool DNA Kit, and the protocol was followed with the addition of lysozyme with an extra 30 minute incubation at 37 degrees Celcius, between steps 2 and 3.

### 3.2.1 16S rRNA gene tag experiment

DNA was amplified by PCR using the Earth Microbiome V4 primer set [12], with the addition of combinatorial in-line barcodes so that all the samples could be sequenced in the same sequencing run [33]. The DNA was sequenced on the Illumina MiSeq platform with paired end 220 nucleotide reads, producing 25 million reads in total.

Reads were overlapped with Pandaseq [58], clustered into Operational Taxonomic Units (OTUs) using UCLUST [23], and annotated with the SILVA database [74] using mothur [79], producing a table of counts per operational taxonomic unit per sample. Twelve milion (48%) of the reads were succesfully overlapped and annotated into 232 OTUs. Differential abundance was analyzed using ALDEEx2 [27].

A generalized workflow for processing 16S rRNA gene sequencing reads is available at [https://github.com/ggloor/miseq\\_bin](https://github.com/ggloor/miseq_bin). The workflow for the 16S rRNA gene tag experiment analysis from the count table stage is on GitHub: [https://github.com/ruthgrace/nafld\\_metaphlan\\_pca](https://github.com/ruthgrace/nafld_metaphlan_pca).

### 3.2.2 MetaPhlAn

MetaPhlAn (Metagenomic Phylogenetic Analysis) [81] is a piece of software that allows one to infer the taxa present based on the metagenomic sequencing experiment. We used this to generate a count table per taxa per sample, and will compare it to our experimental results from the 16S rRNA gene tag sequencing experiment.

The MetaPhlAn tutorial ([https://bitbucket.org/nsegata/metaphlan/wiki/MetaPhlAn\\_Pipelines\\_Tutorial](https://bitbucket.org/nsegata/metaphlan/wiki/MetaPhlAn_Pipelines_Tutorial)) was followed, using an additional marker<sub>count</sub> option in the `merge_metaphlan_table.py`

### 3.2.3 Metagenomic experiment

A metagenomic sequencing experiment was performed using total bacterial DNA from 10 healthy controls and 10 of the patients with NASH. Samples from healthy patients were selected to exclude confounding factors. Samples from NASH patients were selected for the most extreme NASH phenotype, and had higher effect sizes in the 16S rRNA gene tag experiment than the full NASH group.

The DNA was sequenced on the Illumina HiSeq platform, with single end 100 nucleotide reads. Samples were barcoded and sequenced on the same sequencing run. After sequencing, the reads were quality filtered and demultiplexed to separate the reads for each sample, yielding nearly 2 billion reads in total.

We used a two pronged strategy to annotate the reads:

First, we created a reference library using the inferred taxa from the 16S rRNA gene tag experiment. For each genus observed we randomly picked 10 strain genomes from the NCBI bacterial genome database. For genera with less than 10 fully sequenced representatives, we selected all available genomes. The library was made with 1134 genomes from 104 bacterial genera. The open reading frame (ORF) library was then clustered at 99% identity for each genus using CD-HIT [48] to decrease the number of ORFs in the library from 3,495,887 to 2,256,844. Annotation was performed with the SEED database [65], and sequenced reads were mapped onto this ORF library. Out of approximately 2 billion reads total, 58.5 million (30.6%) were mapped by this method, over 5836 unique SEED hierarchy annotations. The primary limitation of this method is a lack of annotated bacterial sequences. The code for the reference library creation and annotation is on GitHub.

Second, we assembled the reads per sample de novo using Trinity [37], producing 8847816 sequences, and removed sequences that matched our reference library with 90% identity as determined by BLAST [2], leaving 5,876,423 sequences. [FILL IN THIS] of these assembled sequences were successfully annotated with the SEED database [65], and sequenced reads were mapped onto this. [FILL IN THIS] additional reads were annotated by this method, over [FILL

<b>Study inclusion criteria</b>
BMI > 40 kg/m <sup>2</sup>
or BMI > 35-40 kg/m <sup>2</sup> with severe weight loss responsive comorbidities, i.e. DM2, hypertension, hyperlipidemia, sleep apnea
and/or gastroesophageal reflux disease
or physical problems interfering with lifestyle
and who have been assessed by the multidisciplinary bariatric team as suitable candidates for laparoscopic RYGB
Male and female
Age 18 years or older
Alcohol consumption ≥20g/d
If known to have hyperlipidemia or DM2, need to be stable drug regimen for at least 3 months prior to study entry
<b>Study exclusion criteria</b>
Liver disease of other etiology
Advanced liver disease (need for liver transplantation in one year or complications such as variceal bleeding, ascites or jaundice)
Abnormal coagulation or other reasons contraindicating a liver biopsy
Medications known to precipitate steatohepatitis 6 months prior to entry
Regular intake of non-steroidal anti-inflammatory drugs; prebiotics, probiotics or antibiotics, ursodeoxycholic acid or any experimental drug in the 3 months prior to study entry
Type 1 diabetes
Chronic gastrointestinal diseases
Previous gastrointestinal surgery modifying the anatomy (prior to bariatric surgery)
Smoking
Pregnancy or breastfeeding
Patients not tolerating Optifast, which is a standard weight loss diet given to all patients pre-bariatric surgery

Table 3.1: **List of overall study inclusion and exclusion criteria.** This table lists the inclusion and exclusion criteria for the 16S rRNA gene tag experiment.

IN THIS] unique SEED hierarchy annotations. The code for the custom assembly pipeline is on GitHub. The data from both prongs was amalgamated into a single table of counts per annotation per sample.

Differential abundance was analyzed using ALDEx2 [27]. A full description of the workflow for this process is included in Appendix A.

<b>Study inclusion criteria</b>
NASH severity
<b>Study exclusion criteria</b>
Took antibiotics at any point
Started Optifast diet early
Sample not frozen immediately after collection
Blood glucose over 7.8 mmol/l

Table 3.2: **List of inclusion and exclusion criteria for metagenomic study.** Patients were selected for the metagenomic study out of the patients selected for the 16S rRNA gene tag sequencing study with the following criteria. Ten healthy and ten patients with NASH were selected in total.

## 3.3 Results

### 3.3.1 16S rRNA gene tag experiment

The top four genus detected by 16S rRNA gene sequencing (excluding unclassified bacteria) were: *Bacteroides*, *Faecalibacterium*, *Blautia*, and *Pseudobutyribrio* (Fig. 3.3.1).

No obvious structure or separation is evident from the principal components analysis in Fig. 3.3.1 or the principal coordinate analysis in Fig. 3.3.1. Furthermore the variance explained by each principal component axis is not notably high, indicating a rather uniform data set. Additionally, no OTUs are significantly differentially abundant between groups (Fig. 3.3.1)

When comparing all the healthy samples with all the NASH samples, the genus with the highest effect sizes are *Adlercreutzia*, *Odoribacter*, and *Escherichia-Shigella*. However, when only the select 10 healthy samples and the 10 extreme NASH samples used in the metagenomic study are compared, the genus with the highest effect sizes are *Ruminococcus*, *Adlercreutzia*, and *Alistipes*. This corresponds with the qPCR experiment, where *Bacteriodetes*, *Prevotella*, and *Ruminococcus* were tested, and only *Ruminococcus* was found to be differentially abundant.

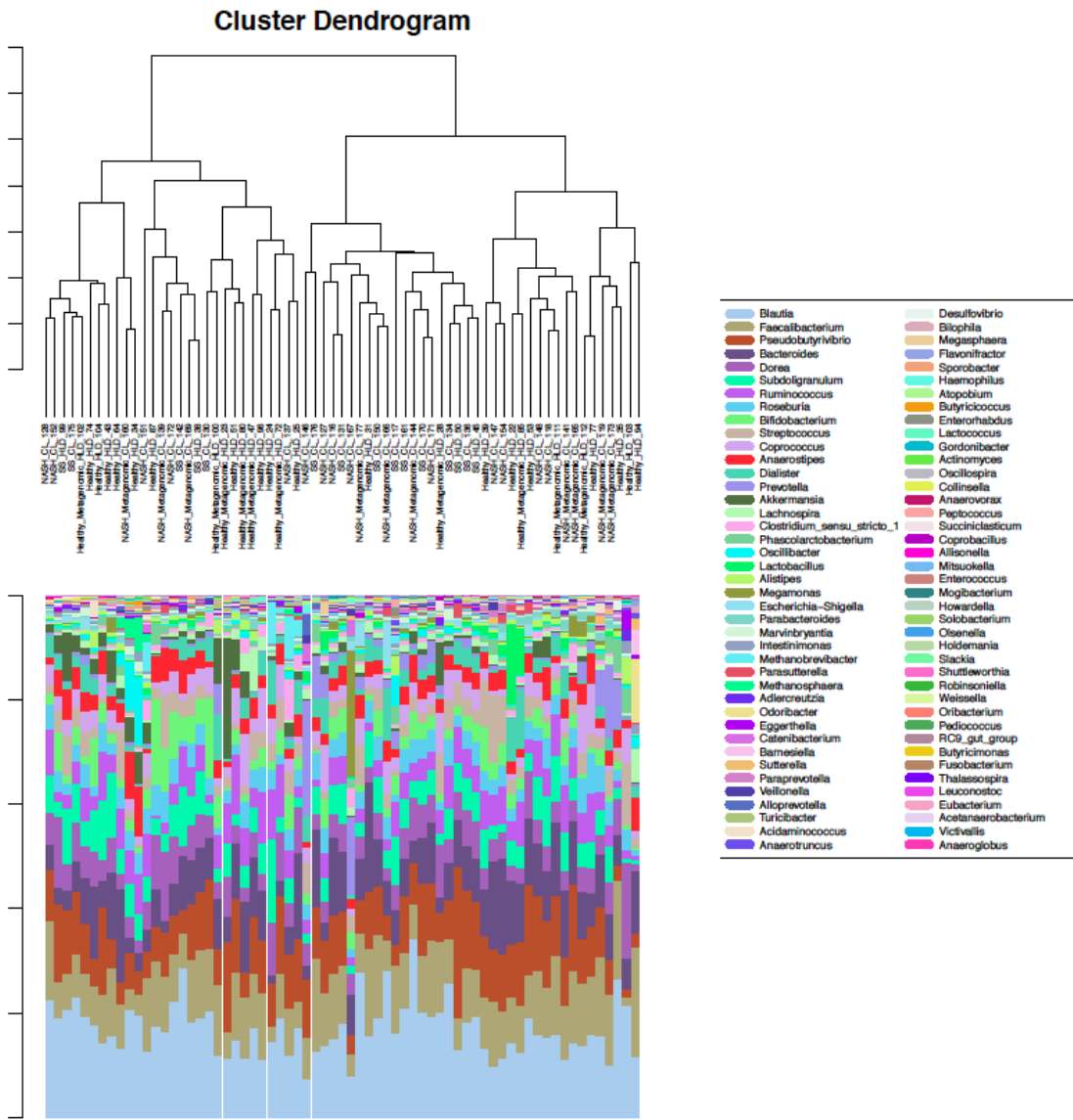


**Figure 3.2: 16S rRNA gene tag sequencing per sample bar plot.** Each column of this bar plot represents one sample, and each color represents one bacterial genus. Genus are listed in the legend in order of decreasing total abundance across all samples. Samples do not cluster according to their condition (healthy, simple steatosis, or nonalcoholic steatohepatitis). Note that OTUs that mapped to unclassified or *Incultae Sedis* were removed, and these made up just over a third of the total abundance.

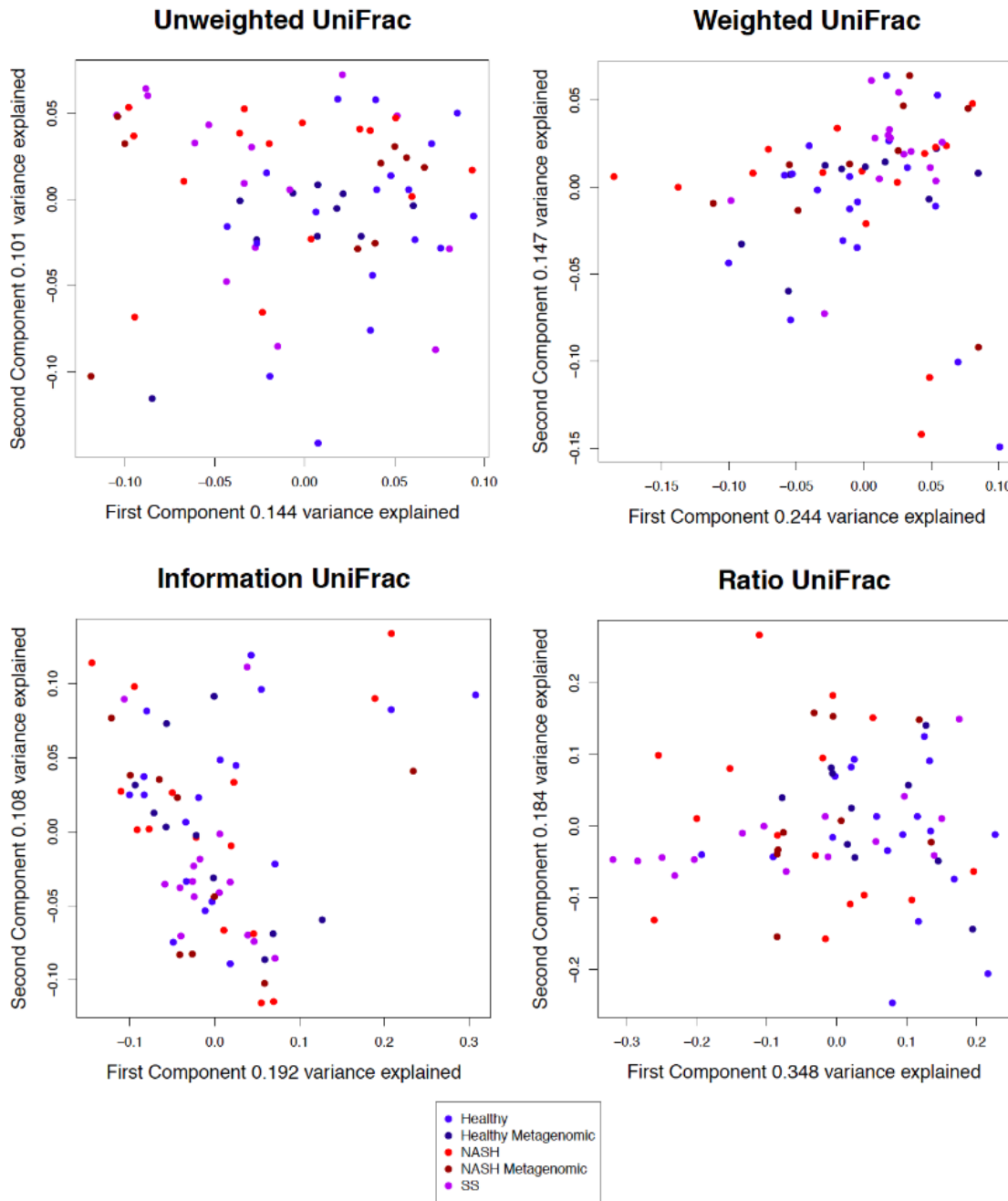


**Figure 3.3: Principal Components Analysis of 16S rRNA gene tag sequencing data with different UniFrac weightings.** Each point represents one sample, and the distances between the samples have been calculated using different UniFrac metrics, taking into account phylogenetic as well as abundance information. There is no obvious separation between groups by any of the UniFrac weightings. Furthermore the variance explained by each principal component axis is not notably high, indicating a rather uniform data set.

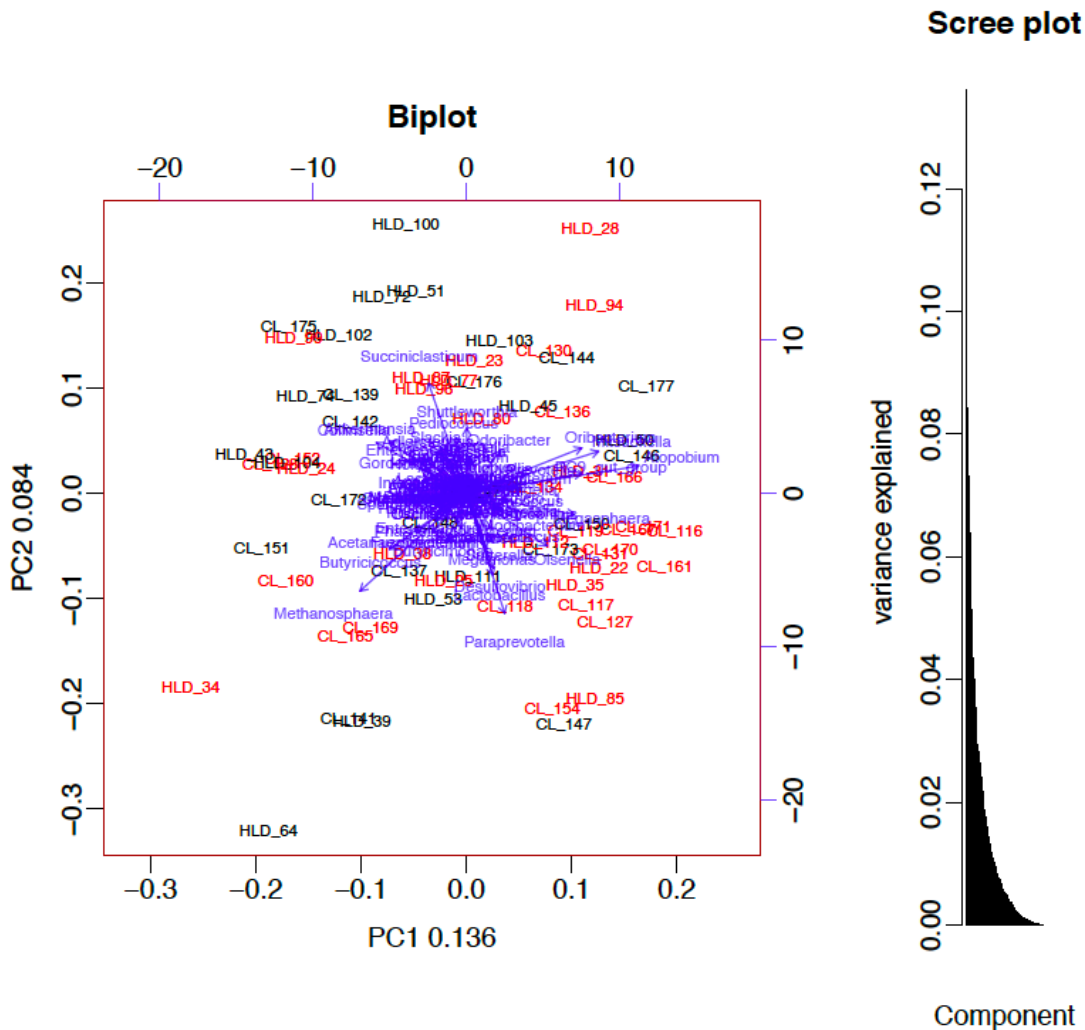


**Figure 3.4: 16S rRNA gene tag sequencing experiment biplot.** Compositional data analysis is done by transforming the counts with a centered log ratio transform, and then performing a principal coordinate analysis. The variance explained by each genus is overlayed on the same principal coordinate analysis plot. Note that the variance explained by the first and the second coordinate is 9% and 8% respectively, indicating that there is not a clear unidirectional separation between groups. Samples from healthy controls are colored black while samples from patients with NASH are colored red.

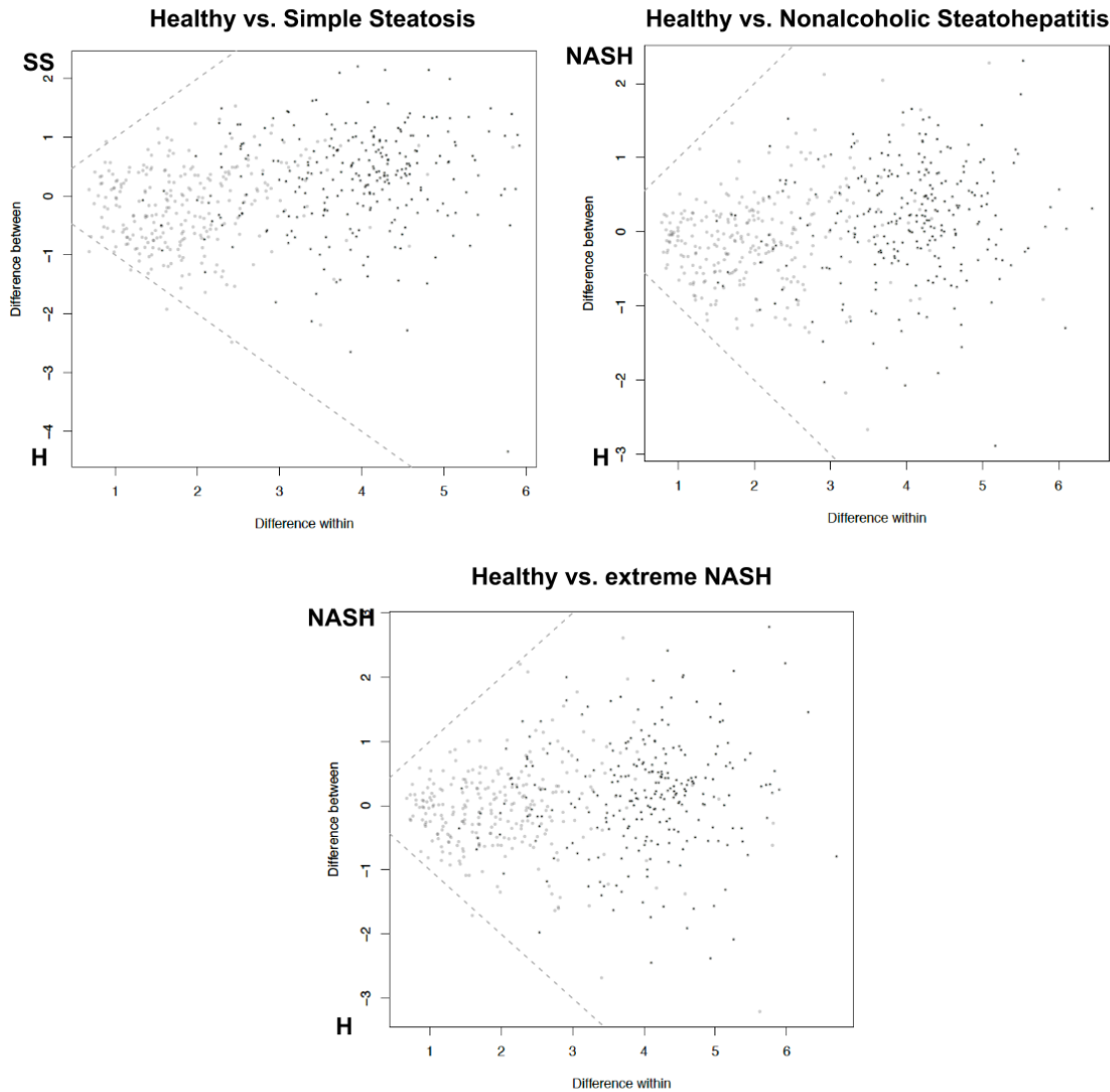


**Figure 3.5: Difference within vs. difference between groups.** Each point represents one OTU, and the differential abundance of that OTU within groups is plotted against the differential abundance between groups. None of the OTUs are more different between groups than within groups. The healthy samples used for these comparisons are the 10 healthy samples used for the metagenomic study. The extreme NASH samples used for these comparisons are the subset of the NASH patients selected for the metegenomic study.

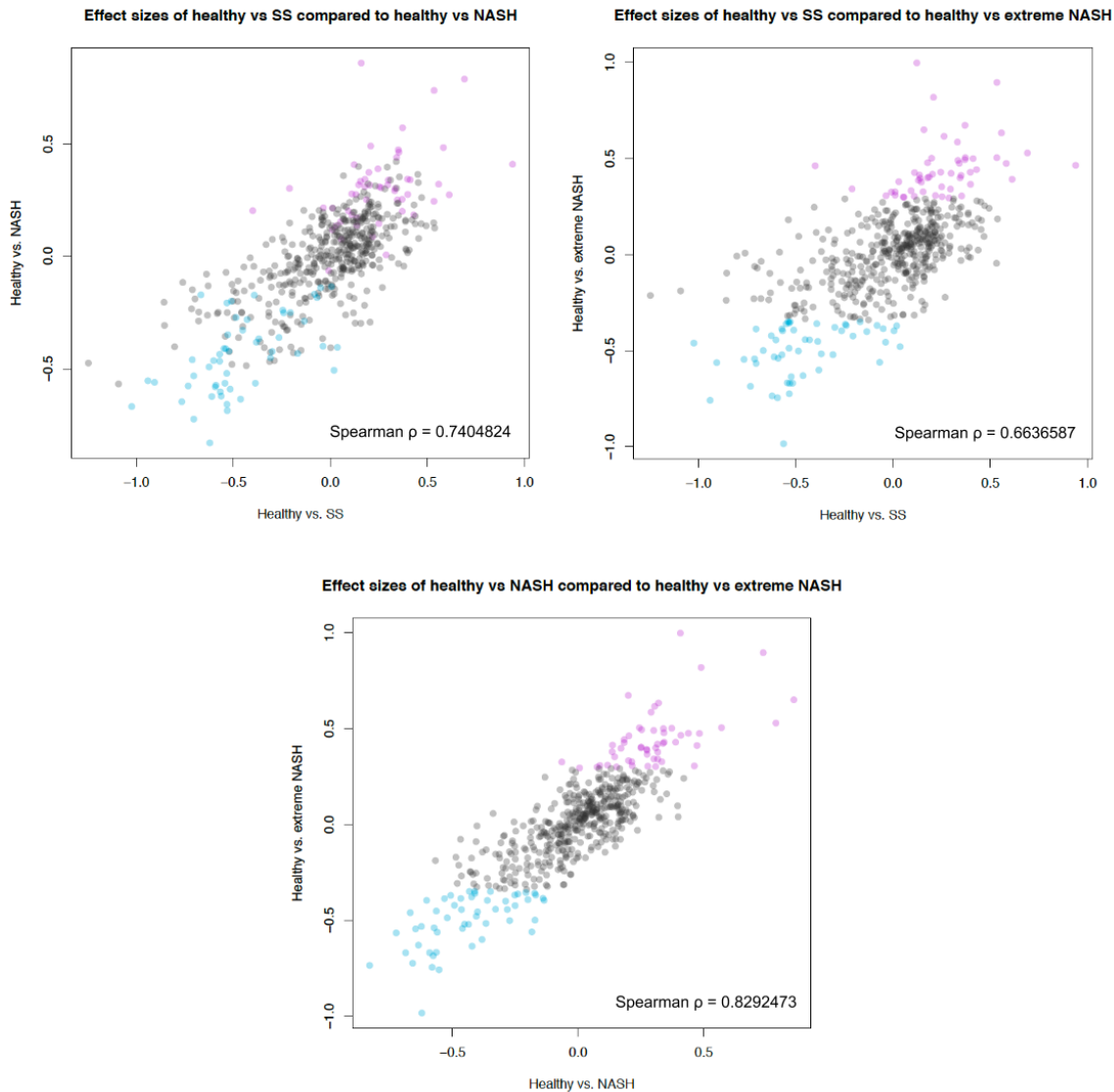


**Figure 3.6: Correlation in effect sizes of different group experiments.** Each point represents one OTU, and the effect size of that OTU in one comparison (for example, comparing the gut microbiome of healthy patients with patients who have simple steatosis) is plotted against the effect size of that OTU in another comparison. The healthy samples used for these comparisons are the 10 healthy samples used for the metagenomic study. The extreme NASH samples used for these comparisons are the subset of the NASH patients selected for the metagenomic study. The median difference in the absolute effect sizes is -0.005547 for Healthy vs. NASH - Healthy vs. SS, 0.01094 for Healthy vs. extreme NASH - Healthy vs. SS, and 0.03105 for Healthy vs. extreme NASH - Healthy vs. NASH. The top decile of OTUs relatively increased in NASH for the metagenomic experiment are colored pink, and the top decile of OTUs relatively increased healthy for the metagenomic experiment are colored blue.

A differential expression analysis performed with ALDEx2 between healthy vs. SS, healthy vs. NASH, and the 10 healthy samples selected for the metagenomic study vs. the 10 NASH samples for the metagenomic study yielded no significantly differentially abundant OTUs (Fig. 3.3.1). However, the effect size (difference between groups divided by the difference within groups) of each OTU in each comparison is correlated (Fig. 3.3.1). The effect sizes are higher in the Healthy vs. extreme NASH compared to the Healthy vs. SS or Healthy vs. NASH comparison.

OTU family	OTU genus	SILVA bootstrap value	H Vs. NASH metagenomic study effect sizes	H Vs. SS effect sizes	H vs. NASH effect sizes	16S genus effect sizes	MetaPhlAn effect sizes
Acidaminococcaceae	Phascolarctobacterium	100	0.998	0.122	0.407	0.827	0.081
Lactobacillaceae	Lactobacillus	97	0.896	0.534	0.736	0.587	-0.899
Prevotellaceae	Paraprevotella	100	0.819	0.208	0.489	0.843	0.064
Lachnospiraceae	Incetrae Sedis	98	0.673	0.37	0.2	NA	NA
Lachnospiraceae	Marvinbryantia	77	0.65	0.159	0.858	0.077	0.269
Lachnospiraceae	Incetrae Sedis	73	0.634	0.557	0.32	NA	NA
Bifidobacteriaceae	Bifidobacterium	100	0.616	0.262	0.304	0.188	0.032
Ruminococcaceae	Incetrae Sedis	72	0.586	0.331	0.291	NA	NA
Prevotellaceae	Paraprevotella	100	0.529	0.691	0.787	0.843	0.064
Lachnospiraceae	unclassified	100	0.505	0.371	0.571	NA	NA
unclassified	unclassified	72	0.505	0.533	0.244	NA	NA
Ruminococcaceae	Butyricoccus	71	0.502	0.198	0.372	0.449	0.28
Lachnospiraceae	Incetrae Sedis	91	0.5	0.411	0.339	NA	NA
Ruminococcaceae	Ruminococcus	93	0.494	0.369	0.253	-0.866	0.023
Coriobacteriaceae	unclassified	97	0.491	0.334	0.301	NA	NA
Lachnospiraceae	unclassified	98	0.478	0.178	0.341	NA	NA
Lactobacillaceae	Lactobacillus	98	0.476	0.341	0.439	0.587	-0.899
Ruminococcaceae	Subdoligranulum	87	0.475	0.582	0.483	-0.087	-0.177
Ruminococcaceae	Incetrae Sedis	98	0.465	0.939	0.409	NA	NA
Ruminococcaceae	unclassified	100	0.462	-0.4	0.202	NA	NA
Coriobacteriaceae	Olsenella	91	0.443	0.429	0.183	0.318	0.141
Ruminococcaceae	Subdoligranulum	98	0.429	0.245	0.388	-0.087	-0.177
Lachnospiraceae	unclassified	100	0.429	0.397	0.342	NA	NA
Prevotellaceae	Prevotella	99	0.427	0.111	0.183	0.212	0.188
Lachnospiraceae	Anaerostipes	100	0.423	0.298	0.338	0.244	0.344
Prevotellaceae	unclassified	70	0.419	0.203	0.316	NA	NA
unclassified	unclassified	92	0.414	0.136	0.137	NA	NA
Ruminococcaceae	Incetrae Sedis	99	0.412	0.35	0.473	NA	NA
Ruminococcaceae	Faecalibacterium	100	0.404	0.185	0.251	-0.226	-0.173
Alcaligenaceae	Sutterella	100	0.4	0.177	0.309	0.162	0.051
unclassified	unclassified	73	0.4	0.345	0.25	NA	NA
Rikenellaceae	Alistipes	100	0.397	0.139	0.17	-0.687	0.053
Lachnospiraceae	Roseburia	98	0.392	0.612	0.273	0.18	0.168
Prevotellaceae	unclassified	75	0.387	0.131	0.274	NA	NA
Coriobacteriaceae	Enterorhabdus	72	0.38	0.029	0.135	0.429	0.224
Ruminococcaceae	Ruminococcus	100	0.378	0.146	0.317	-0.866	0.023
unclassified	unclassified	98	0.366	0.398	0.275	NA	NA
Veillonellaceae	Dialister	100	0.353	0.25	0.145	-0.297	-0.038
Lachnospiraceae	unclassified	100	0.342	-0.211	0.301	NA	NA
Family XIII	Incetrae Sedis	100	0.341	0.295	0.317	NA	NA
Bacteroidaceae	Bacteroides	100	0.333	0.093	0.201	-0.356	-0.124
Lachnospiraceae	unclassified	100	0.327	0.155	0.333	NA	NA
Lachnospiraceae	unclassified	100	0.327	0.01	0.214	NA	NA
Desulfovibrionaceae	Desulfovibrio	100	0.326	-0.009	-0.065	0.283	0.046
Lachnospiraceae	unclassified	100	0.309	0.011	0.117	NA	NA
Lachnospiraceae	Blautia	96	0.308	0.218	0.087	-0.031	0.192
Lachnospiraceae	Blautia	97	0.306	-0.036	0.215	-0.031	0.192
Ruminococcaceae	unclassified	100	0.305	0.353	0.462	NA	NA
Christensenellaceae	unclassified	99	0.303	0.11	0.277	NA	NA
Alcaligenaceae	Parasutterella	100	0.302	0.252	0.308	0.389	0.521
Lachnospiraceae	Incetrae Sedis	100	0.3	0.052	0.153	NA	NA
Ruminococcaceae	Subdoligranulum	92	0.299	0.056	0.076	-0.087	-0.177
Acidaminococcaceae	Acidaminococcus	100	0.295	0.287	0.006	0.345	-0.737

**Table 3.3: Top decile of OTUs relatively increased in NASH based on effect size from healthy vs. NASH comparison.** This table lists the OTUs, their effect sizes in all the comparisons, as well as the corresponding genus-level effect sizes in the 16S rRNA gene tag experiment and MetaPhlAn comparisons between the 10 healthy and 10 NASH samples selected for the metagenomic study. The OTUs were picked by open reference, by clustering and comparison with the SILVA database [74]. Positive effect sizes indicate that the feature was found to be relatively increased in NASH while negative effect sizes indicate that the feature was found to be relatively increased in healthy. OTUs were annotated with SILVA, and a confidence percentage is reported based on the provided bootstrapping algorithm. *Incetrae Sedis* and unclassified genera were not analyzed at the genus level.

OTU family	OTU genus	SILVA bootstrap value	H Vs. NASH metagenomic study effect sizes	H Vs. SS effect sizes	H vs. NASH effect sizes	16S genus effect sizes	MetaPhlAn effect sizes
Ruminococcaceae	Incertae Sedis	100	-0.349	-0.539	-0.411	NA	NA
Verrucomicrobiaceae	Akkermansia	100	-0.35	-0.169	-0.433	-0.496 0.343	
Porphyromonadaceae	Parabacteroides	100	-0.35	-0.529	-0.349	-0.313 0.016	
Rikenellaceae	Alistipes	100	-0.356	-0.534	-0.208	-0.687 0.053	
Lachnospiraceae	Incertae Sedis	73	-0.36	-0.392	-0.173	NA	NA
Lachnospiraceae	unclassified	100	-0.361	-0.549	-0.411	NA	NA
Streptococcaceae	Streptococcus	100	-0.363	-0.245	-0.24	-0.18 0.233	
Lachnospiraceae	unclassified	100	-0.369	-0.082	-0.169	NA	NA
Lachnospiraceae	Dorea	100	-0.369	-0.241	-0.252	-0.267 -0.154	
Lachnospiraceae	Roseburia	83	-0.371	0.019	-0.507	0.18 0.168	
Lachnospiraceae	Incertae Sedis	82	-0.379	-0.3	-0.424	NA	NA
Christensenellaceae	unclassified	98	-0.386	-0.051	-0.14	NA	NA
Christensenellaceae	unclassified	100	-0.387	-0.571	-0.467	NA	NA
Lachnospiraceae	Blautia	93	-0.387	-0.704	-0.532	-0.031 0.192	
Ruminococcaceae	unclassified	100	-0.393	-0.511	-0.2	NA	NA
Lachnospiraceae	Roseburia	91	-0.397	-0.568	-0.603	0.18 0.168	
Porphyromonadaceae	Odoribacter	100	-0.397	0.005	-0.135	-0.541 -0.333	
Lachnospiraceae	Incertae Sedis	85	-0.397	-0.265	-0.362	NA	NA
Lachnospiraceae	unclassified	98	-0.401	-0.135	-0.289	NA	NA
Porphyromonadaceae	Odoribacter	100	-0.422	-0.625	-0.492	-0.541 -0.333	
Erysipelotrichaceae	Turicibacter	100	-0.424	-0.206	-0.251	-0.52 -0.717	
Christensenellaceae	unclassified	100	-0.443	-0.452	-0.329	NA	NA
Ruminococcaceae	Ruminococcus	100	-0.444	-0.429	-0.282	-0.866 0.023	
Christensenellaceae	unclassified	99	-0.445	-0.602	-0.464	NA	NA
Lachnospiraceae	unclassified	100	-0.452	-0.387	-0.564	NA	NA
Bacteroidaceae	Bacteroides	100	-0.456	-0.038	-0.4	-0.356 -0.124	
Ruminococcaceae	Incertae Sedis	84	-0.461	-1.024	-0.668	NA	NA
Veillonellaceae	Dialister	100	-0.479	0.036	-0.405	-0.297 -0.038	
Bacteroidaceae	Bacteroides	100	-0.488	-0.534	-0.521	-0.356 -0.124	
Prevotellaceae	Alloprevotella	100	-0.5	-0.667	-0.172	-0.001 0.863	
Bacteroidaceae	Bacteroides	100	-0.502	-0.487	-0.272	-0.356 -0.124	
Rikenellaceae	Alistipes	100	-0.517	-0.369	-0.367	-0.687 0.053	
Coriobacteriaceae	Adlercreutzia	100	-0.521	-0.309	-0.452	-0.372 -0.298	
Ruminococcaceae	unclassified	100	-0.522	-0.571	-0.436	NA	NA
Family XIII	Anaerovorax	91	-0.533	-0.611	-0.624	-0.476 -0.152	
Ruminococcaceae	unclassified	76	-0.54	-0.59	-0.573	NA	NA
Lachnospiraceae	Pseudobutyryvibrio	98	-0.543	-0.712	-0.46	-0.423 -0.091	
Bacteroidaceae	Bacteroides	100	-0.546	-0.766	-0.647	-0.356 -0.124	
Bacteroidaceae	Bacteroides	100	-0.561	-0.069	-0.184	-0.356 -0.124	
Lachnospiraceae	Blautia	85	-0.562	-0.906	-0.561	-0.031 0.192	
Ruminococcaceae	Faecalibacterium	100	-0.566	-0.704	-0.724	-0.226 -0.173	
unclassified	unclassified	85	-0.601	-0.381	-0.382	NA	NA
Ruminococcaceae	Incertae Sedis	100	-0.63	-0.463	-0.635	NA	NA
Ruminococcaceae	Subdoligranulum	99	-0.636	-0.523	-0.422	-0.087 -0.177	
Ruminococcaceae	Incertae Sedis	97	-0.668	-0.544	-0.565	NA	NA
Ruminococcaceae	Ruminococcus	100	-0.669	-0.516	-0.591	-0.866 0.023	
Lachnospiraceae	Incertae Sedis	85	-0.67	-0.532	-0.686	NA	NA
Lachnospiraceae	Coprococcus	91	-0.686	-0.733	-0.577	-0.647 0.469	
Ruminococcaceae	unclassified	74	-0.725	-0.533	-0.658	NA	NA
Erysipelotrichaceae	unclassified	100	-0.736	-0.621	-0.83	NA	NA
Ruminococcaceae	Subdoligranulum	85	-0.746	-0.594	-0.581	-0.087 -0.177	
Lachnospiraceae	Dorea	100	-0.759	-0.94	-0.554	-0.267 -0.154	
Family XIII	Incertae Sedis	91	-0.985	-0.563	-0.622	NA	NA

**Table 3.4: Bottom decile of OTUs relatively increased in healthy based on effect size from healthy vs. NASH comparison.** This table lists the OTUs, their effect sizes in all the comparisons, as well as the corresponding genus-level effect sizes in the 16S rRNA gene tag experiment and MetaPhlAn comparisons between the 10 healthy and 10 NASH samples selected for the metagenomic study. The OTUs were picked by open reference, by clustering and comparison with the SILVA database [74]. Positive effect sizes indicate that the feature was found to be relatively increased in NASH while negative effect sizes indicate that the feature was found to be relatively increased in healthy. OTUs were annotated with SILVA, and a confidence percentage is reported based on the provided bootstrapping algorithm. *Incertae Sedis* and unclassified genera were not analyzed at the genus level.

### 3.3.2 Metagenomic experiment

#### MetaPhlAn

We ran the metagenomic sequences through MetaPhlAn to infer what the results would be with 16S rRNA gene tag sequencing, so that we could compare with our empirical 16S rRNA gene tag sequencing results. The effect size Spearman coefficient (Fig. 3.3.2) is smaller than the effect size coefficient between the healthy vs. SS and healthy vs. NASH comparison, even though in this case the same samples are being compared.

The operational taxonomic units in the MetaPhlAn and 16S rRNA gene analysis were derived from different databases, and could not be compared directly, so the effect size comparison in Fig. 3.3.2 was done at the genus level. Note that OTUs can reside in between genera, such that the genus classification is not perfectly concordant between the two comparisons. The top four relatively abundant genera from the MetaPhlAn analysis were *Ruminococcus*, *Eubacterium*, *Coprococcus*, and *Bacteroides*. Only *Bacteroides* is also on the top four relatively abundant genera from the 16S rRNA gene tag sequencing experiment.

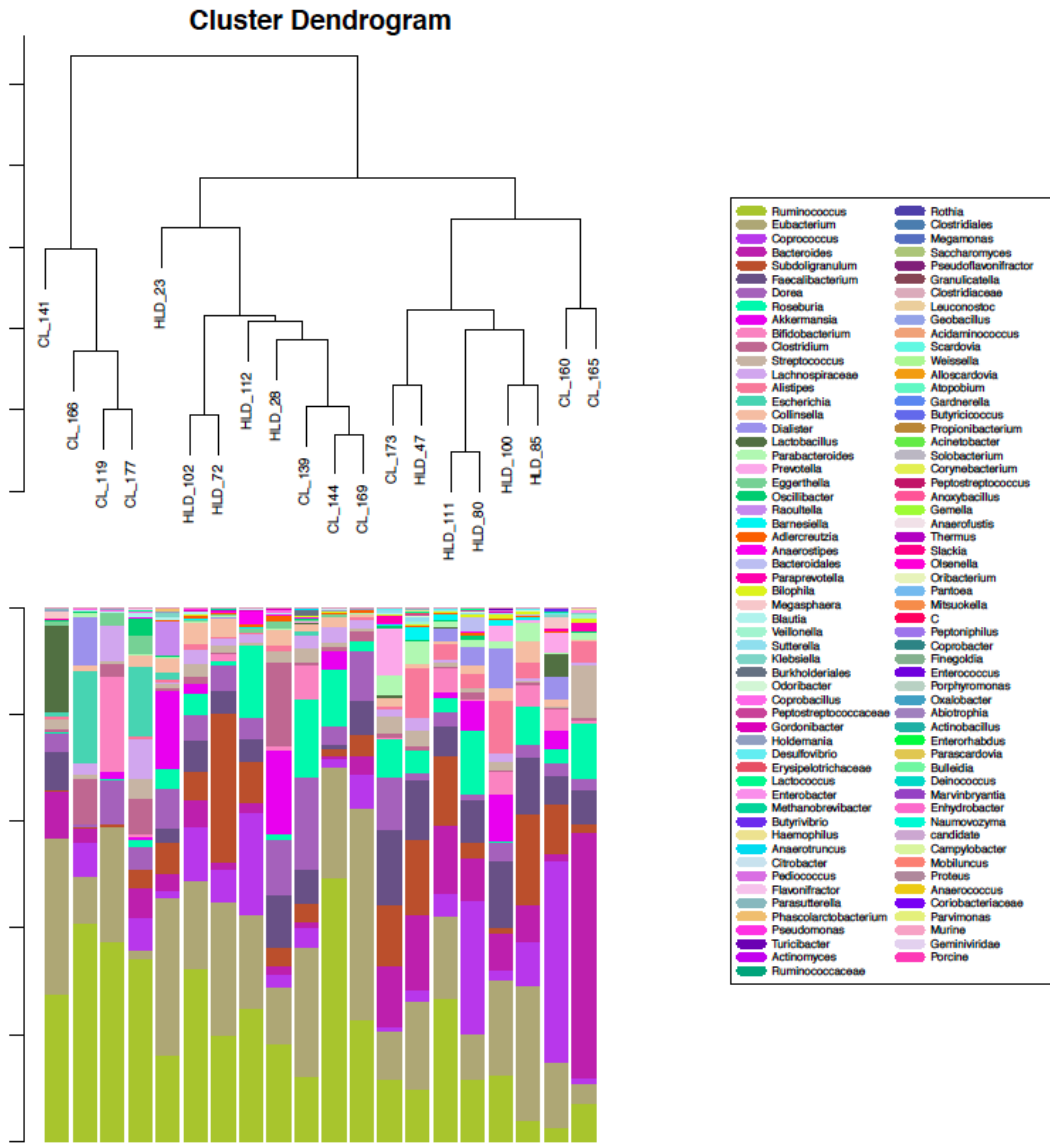


**Figure 3.7: Taxa barplot dendrogram derived from MetaPhlAn.** The metagenomic reads were input into MetaPhlAn to generate a count table. The taxa in the count table were filtered such that only taxa with at least 1% abundance in any sample was kept. In this barplot, each bar represents one sample, and each color represents one genus, with the size of the colored segments corresponding with the relative abundance of the genus.

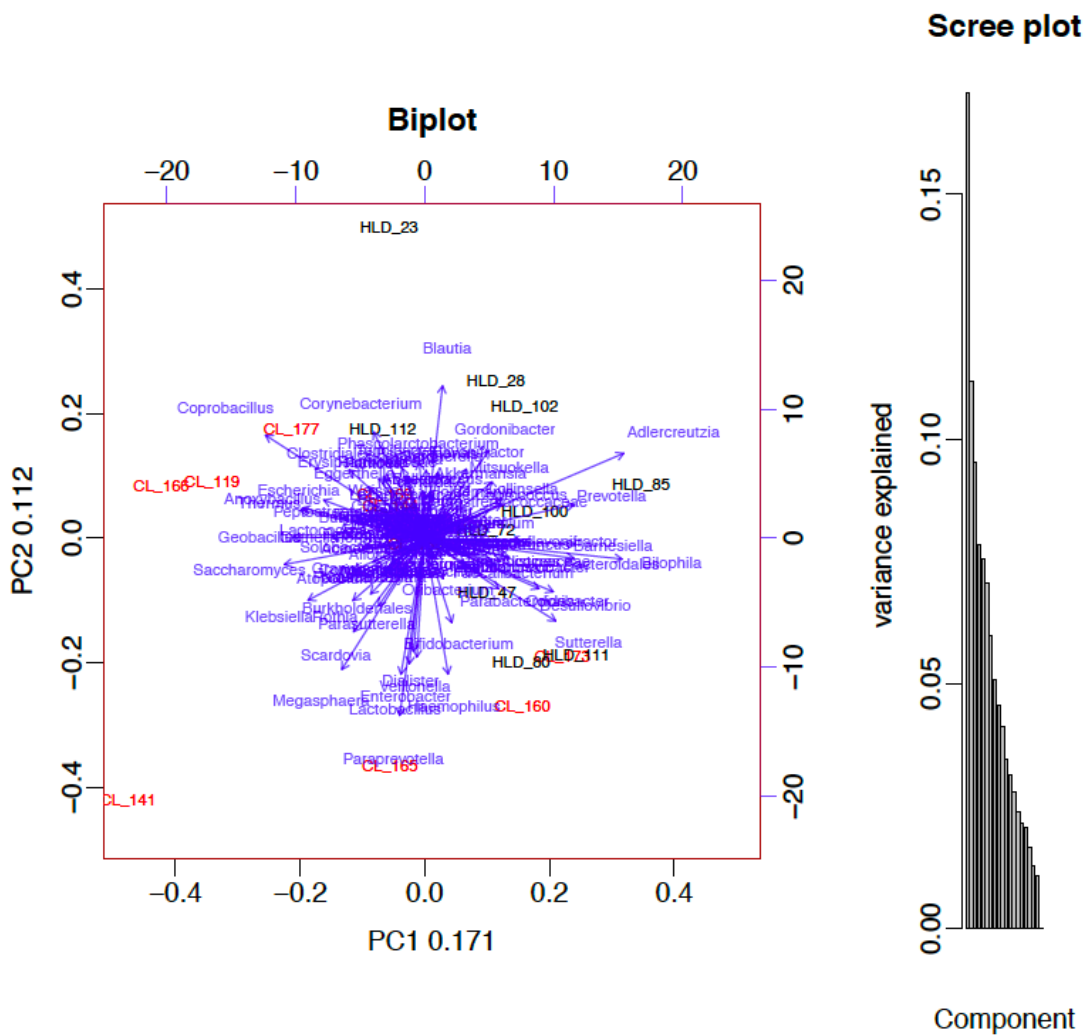
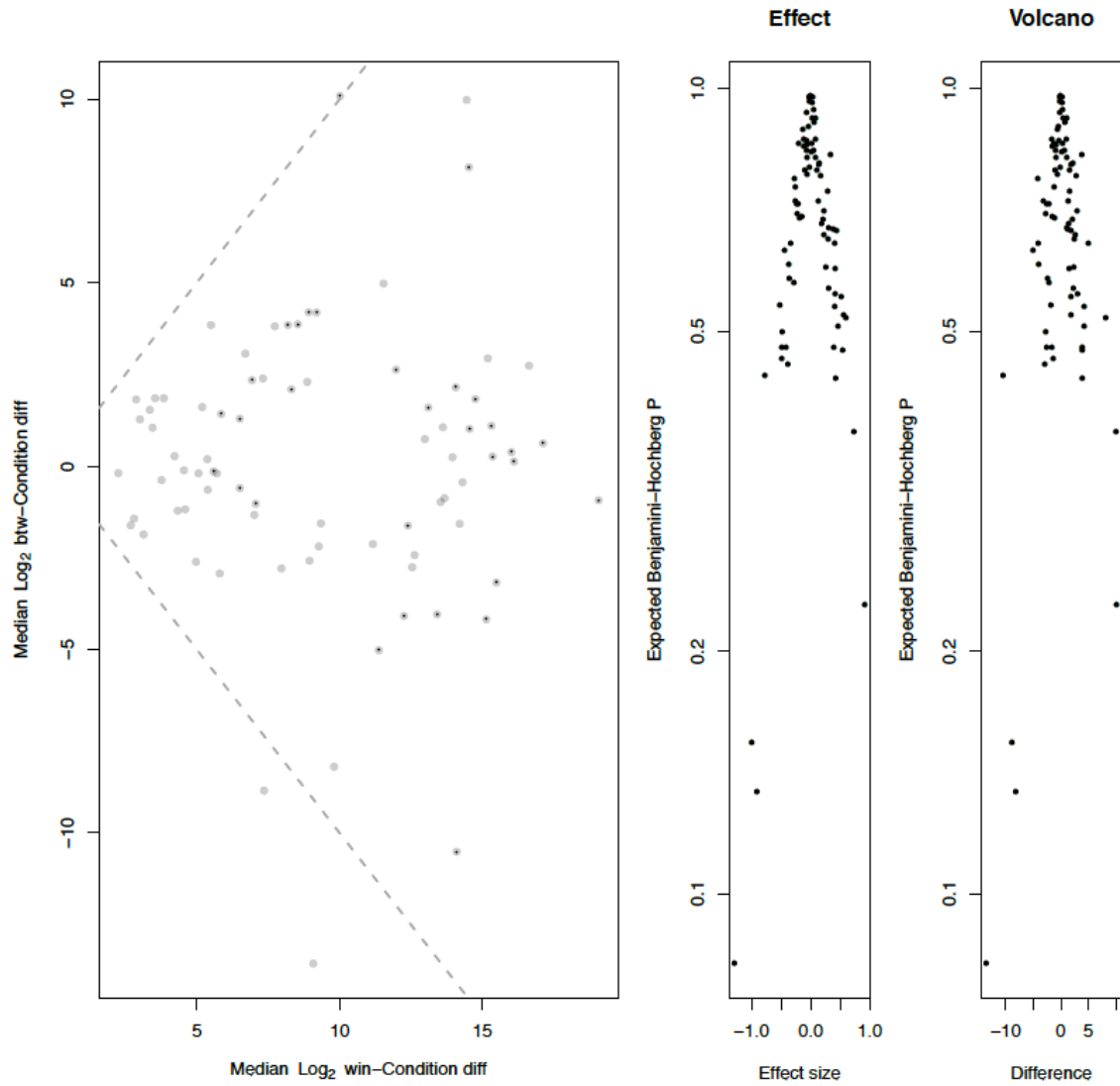
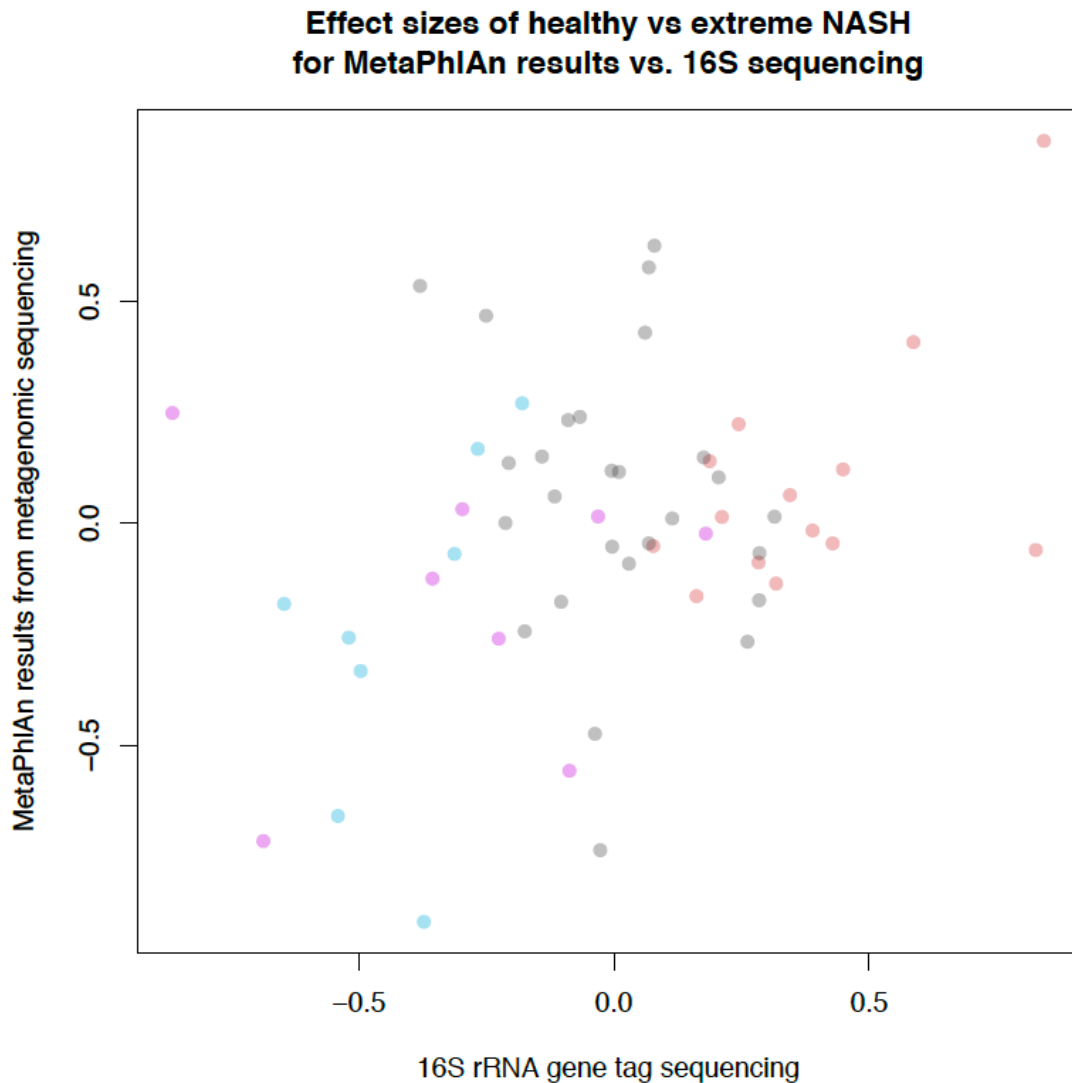


Figure 3.8: **Biplot derived from MetaPhlAn.** Compositional data analysis is done by transforming the counts with a centered log ratio transform, and then performing a principal coordinate analysis. The variance explained by each genera is overlayed on the same principal coordinate analysis plot. This biplot was generated from the count table inferred by MetaPhlAn, with taxa filtered such that only taxa with at least 1% abundance in any sample was kept. Note that the variance explained by the first and the second coordinate is 17% and 11% respectively, indicating that there is not a clear unidirectional separation between groups. Samples from healthy controls are colored black while samples from patients with NASH are colored red.



**Figure 3.9: Difference within groups vs. difference between groups per taxa, derived from MetaPhlAn.** This plot was generated from the count table inferred by MetaPhlAn, with taxa filtered such that only taxa with at least 1% abundance in any sample was kept. No taxa are more differential between groups than within groups. A positive difference between indicates that the taxa was relatively increased in NASH while a negative difference between indicates that the taxa was relatively increased in healthy. This analysis was done at the OTU level.



**Figure 3.10: Effect size correlation between MetaPhiAn and 16S rRNA gene tag sequencing.** For this plot, taxa were amalgamated at the genus level. The effect sizes for the comparison of the healthy and NASH samples selected for the metagenomic study are shown. The Spearman coefficient is 0.2021001. Genera corresponding with OTUs identified to have the top deciles of effect sizes in the 16S rRNA gene tag experiment comparison are colored - red for OTUs relatively abundant in NASH, and blue for OTUs relatively abundant in the healthy condition. Genera corresponding to both OTUs in the NASH and healthy deciles are colored purple.

## 3.4 Discussion

Given the inconsistency in the five papers that have been published about NAFLD and the gut microbiome, we have performed our analysis in a rigorous manner in an effort to find OTUs with true effects. We found that there was no significant difference between groups by sample clustering (Fig. 3.3.1) or at the level of the individual OTUs (Fig. 3.3.1).

There are several factors that would make such a study underpowered. First, the gut microbiome is highly diverse between individuals. This is compounded by the fact that the samples were taken from a diverse Toronto population, including people who immigrated from other countries who likely have different diets. The literature shows that differences in the gut microbiome are often driven by diet [17]. Additionally, the nature of microbiome data is that there are very many more variables (in the form of OTUs or annotated gene functions) than samples, and the power of the study is inversely proportional to the number of variables.

From Fig. 3.3.1, the correlation shows that even though there is not enough power to detect a significant difference, the difference from the healthy baseline are moving in the same direction through simple steatosis to nonalcoholic steatohepatitis to extreme NASH.

We hypothesize that there is a characterizable difference in the gut microbiome between patients prone to NASH and healthy controls. Further study with a higher sample size, a more homogenous population, and a greater phenotypic difference between groups may provide the statistical power required to detect the nature of this difference.

# Chapter 4

## Theorems

### 4.1 Basic Theorems

**Theorem 4.1.1**  $e^{i\pi} = -1$

# Bibliography

- [1] John Aitchison. “The statistical analysis of compositional data”. In: *Journal of the Royal Statistical Society. Series B (Methodological)* (1982), pp. 139–177.
- [2] Stephen F Altschul et al. “Basic local alignment search tool”. In: *Journal of molecular biology* 215.3 (1990), pp. 403–410.
- [3] Marti J Anderson and Trevor J Willis. “Canonical analysis of principal coordinates: a useful method of constrained ordination for ecology”. In: *Ecology* 84.2 (2003), pp. 511–525.
- [4] Manimozhiyan Arumugam et al. “Enterotypes of the human gut microbiome”. In: *nature* 473.7346 (2011), pp. 174–180.
- [5] Edward W Beals. “Bray-Curtis ordination: an effective strategy for analysis of multi-variate ecological data”. In: *Advances in Ecological Research* 14.1 (1984), p. 55.
- [6] David R Bentley et al. “Accurate whole human genome sequencing using reversible terminator chemistry”. In: *nature* 456.7218 (2008), pp. 53–59.
- [7] Alain Berson et al. “Steatohepatitis-inducing drugs cause mitochondrial dysfunction and lipid peroxidation in rat hepatocytes”. In: *Gastroenterology* 114.4 (1998), pp. 764–774.
- [8] Jérôme Boursier et al. “The severity of nonalcoholic fatty liver disease is associated with gut dysbiosis and shift in the metabolic function of the gut microbiota”. In: *Hepatology* (2016).
- [9] Benjamin J Callahan et al. “DADA2: High resolution sample inference from amplicon data”. In: *bioRxiv* (2015), p. 024034.
- [10] J Gregory Caporaso et al. “Global patterns of 16S rRNA diversity at a depth of millions of sequences per sample”. In: *Proceedings of the National Academy of Sciences* 108.Supplement 1 (2011), pp. 4516–4522.
- [11] J Gregory Caporaso et al. “QIIME allows analysis of high-throughput community sequencing data”. In: *Nature methods* 7.5 (2010), pp. 335–336.
- [12] J Gregory Caporaso et al. “Ultra-high-throughput microbial community analysis on the Illumina HiSeq and MiSeq platforms”. In: *The ISME journal* 6.8 (2012), pp. 1621–1624.
- [13] Daniel Aguirre de Cárcer et al. “Evaluation of subsampling-based normalization strategies for tagged high-throughput sequencing data sets from gut microbiomes”. In: *Applied and environmental microbiology* 77.24 (2011), pp. 8795–8798.

- [14] Jun Chen et al. “Associating microbiome composition with environmental covariates using generalized UniFrac distances”. In: *Bioinformatics* 28.16 (2012), pp. 2106–2113.
- [15] Francesca D Ciccarelli et al. “Toward automatic reconstruction of a highly resolved tree of life”. In: *science* 311.5765 (2006), pp. 1283–1287.
- [16] James R Cole et al. “The Ribosomal Database Project: improved alignments and new tools for rRNA analysis”. In: *Nucleic acids research* 37.suppl 1 (2009), pp. D141–D145.
- [17] Lawrence A David et al. “Diet rapidly and reproducibly alters the human gut microbiome”. In: *Nature* 505.7484 (2014), pp. 559–563.
- [18] Arthur L Delcher et al. “Identifying bacterial genes and endosymbiont DNA with Glimmer”. In: *Bioinformatics* 23.6 (2007), pp. 673–679.
- [19] Todd Z DeSantis et al. “Greengenes, a chimera-checked 16S rRNA gene database and workbench compatible with ARB”. In: *Applied and environmental microbiology* 72.7 (2006), pp. 5069–5072.
- [20] Julia M Di Bella et al. “High throughput sequencing methods and analysis for microbiome research”. In: *Journal of microbiological methods* 95.3 (2013), pp. 401–414.
- [21] SL Dollhopf, SA Hashsham, and JM Tiedje. “Interpreting 16S rDNA T-RFLP data: application of self-organizing maps and principal component analysis to describe community dynamics and convergence”. In: *Microbial Ecology* 42.4 (2001), pp. 495–505.
- [22] Robert C Edgar. “MUSCLE: multiple sequence alignment with high accuracy and high throughput”. In: *Nucleic acids research* 32.5 (2004), pp. 1792–1797.
- [23] Robert C Edgar. “Search and clustering orders of magnitude faster than BLAST”. In: *Bioinformatics* 26.19 (2010), pp. 2460–2461.
- [24] JJ Egozcue and V Pawlowsky-Glahn. “Evidence information in bayesian updating”. In: *Proceedings of the 4th International Workshop on Compositional Data Analysis*. 2011.
- [25] Steven N Evans and Frederick A Matsen. “The phylogenetic Kantorovich–Rubinstein metric for environmental sequence samples”. In: *Journal of the Royal Statistical Society: Series B (Statistical Methodology)* 74.3 (2012), pp. 569–592.
- [26] Andrew D Fernandes et al. “ANOVA-like differential expression (ALDEx) analysis for mixed population RNA-Seq”. In: *PLoS One* 8.7 (2013), e67019.
- [27] Andrew D Fernandes et al. “Unifying the analysis of high-throughput sequencing datasets: characterizing RNA-seq, 16S rRNA gene sequencing and selective growth experiments by compositional data analysis”. In: *Microbiome* 2.1 (2014), p. 1.
- [28] Harry J Flint et al. “Polysaccharide utilization by gut bacteria: potential for new insights from genomic analysis”. In: *Nature Reviews Microbiology* 6.2 (2008), pp. 121–131.
- [29] DN Fredericks and David A Relman. “Sequence-based identification of microbial pathogens: a reconsideration of Koch’s postulates.” In: *Clinical microbiology reviews* 9.1 (1996), pp. 18–33.
- [30] Jonathan Friedman and Eric J Alm. “Inferring correlation networks from genomic survey data”. In: *PLoS Comput Biol* 8.9 (2012), e1002687.

- [31] Jack A Gilbert, Janet K Jansson, and Rob Knight. “The Earth Microbiome project: successes and aspirations”. In: *BMC biology* 12.1 (2014), p. 69.
- [32] Steven R Gill et al. “Metagenomic analysis of the human distal gut microbiome”. In: *science* 312.5778 (2006), pp. 1355–1359.
- [33] Gregory B Gloor et al. “Microbiome profiling by illumina sequencing of combinatorial sequence-tagged PCR products”. In: *PloS one* 5.10 (2010), e15406.
- [34] Monika A Gorzelak et al. “Methods for Improving Human Gut Microbiome Data by Reducing Variability through Sample Processing and Storage of Stool”. In: *PloS one* 10.8 (2015), e0134802.
- [35] J Graessler et al. “Metagenomic sequencing of the human gut microbiome before and after bariatric surgery in obese patients with type 2 diabetes: correlation with inflammatory and metabolic parameters”. In: *The pharmacogenomics journal* 13.6 (2013), pp. 514–522.
- [36] Francisco Guarner and Juan-R Malagelada. “Gut flora in health and disease”. In: *The Lancet* 361.9356 (2003), pp. 512–519.
- [37] Brian J Haas et al. “De novo transcript sequence reconstruction from RNA-seq using the Trinity platform for reference generation and analysis”. In: *Nature protocols* 8.8 (2013), pp. 1494–1512.
- [38] Elaine Y Hsiao et al. “Microbiota modulate behavioral and physiological abnormalities associated with neurodevelopmental disorders”. In: *Cell* 155.7 (2013), pp. 1451–1463.
- [39] Ruben Hummelen et al. “Deep sequencing of the vaginal microbiota of women with HIV”. In: *PloS one* 5.8 (2010), e12078.
- [40] Weiwei Jiang et al. “Dysbiosis gut microbiota associated with inflammation and impaired mucosal immune function in intestine of humans with non-alcoholic fatty liver disease”. In: *Scientific reports* 5 (2015).
- [41] Minoru Kanehisa and Susumu Goto. “KEGG: kyoto encyclopedia of genes and genomes”. In: *Nucleic acids research* 28.1 (2000), pp. 27–30.
- [42] R Koch. “Über bakteriologische Forschung Verhandlung des X Internationalen Medico-chirurgischen Congresses, Berlin, 1890, 1, 35. August Hirschwald, Berlin”. In: *German.) Xth International Congress of Medicine, Berlin. 1891.*
- [43] Heidi H Kong et al. “Temporal shifts in the skin microbiome associated with disease flares and treatment in children with atopic dermatitis”. In: *Genome research* 22.5 (2012), pp. 850–859.
- [44] HA Krebs and JR Perkins. “The physiological role of liver alcohol dehydrogenase”. In: *Biochemical Journal* 118.4 (1970), pp. 635–644.
- [45] Morgan GI Langille et al. “Predictive functional profiling of microbial communities using 16S rRNA marker gene sequences”. In: *Nature biotechnology* 31.9 (2013), pp. 814–821.
- [46] Ben Langmead and Steven L Salzberg. “Fast gapped-read alignment with Bowtie 2”. In: *Nature methods* 9.4 (2012), pp. 357–359.

- [47] Nadja Larsen et al. “Gut microbiota in human adults with type 2 diabetes differs from non-diabetic adults”. In: *PLoS one* 5.2 (2010), e9085.
- [48] Weizhong Li and Adam Godzik. “Cd-hit: a fast program for clustering and comparing large sets of protein or nucleotide sequences”. In: *Bioinformatics* 22.13 (2006), pp. 1658–1659.
- [49] Michael I Love, Wolfgang Huber, and Simon Anders. “Moderated estimation of fold change and dispersion for RNA-seq data with DESeq2”. In: *Genome biology* 15.12 (2014), pp. 1–21.
- [50] David Lovell et al. “Proportionality: a valid alternative to correlation for relative data”. In: *PLoS Comput Biol* 11.3 (2015), e1004075.
- [51] Catherine A Lozupone et al. “Quantitative and qualitative  $\beta$  diversity measures lead to different insights into factors that structure microbial communities”. In: *Applied and environmental microbiology* 73.5 (2007), pp. 1576–1585.
- [52] Catherine Lozupone and Rob Knight. “UniFrac: a new phylogenetic method for comparing microbial communities”. In: *Applied and environmental microbiology* 71.12 (2005), pp. 8228–8235.
- [53] Catherine Lozupone et al. “UniFrac: an effective distance metric for microbial community comparison”. In: *The ISME journal* 5.2 (2011), p. 169.
- [54] Jean M Macklaim et al. “Comparative meta-RNA-seq of the vaginal microbiota and differential expression by Lactobacillus iners in health and dysbiosis”. In: *Microbiome* 1.1 (2013), p. 1.
- [55] Siddhartha Mandal et al. “Analysis of composition of microbiomes: a novel method for studying microbial composition”. In: *Microbial ecology in health and disease* 26 (2015).
- [56] Janet GM Markle et al. “Sex differences in the gut microbiome drive hormone-dependent regulation of autoimmunity”. In: *Science* 339.6123 (2013), pp. 1084–1088.
- [57] Victor M Markowitz et al. “IMG: the integrated microbial genomes database and comparative analysis system”. In: *Nucleic acids research* 40.D1 (2012), pp. D115–D122.
- [58] Andre P Masella et al. “PANDAseq: paired-end assembler for illumina sequences”. In: *BMC bioinformatics* 13.1 (2012), p. 31.
- [59] NI McNeil. “The contribution of the large intestine to energy supplies in man.” In: *The American journal of clinical nutrition* 39.2 (1984), pp. 338–342.
- [60] Folker Meyer et al. “The metagenomics RAST server—a public resource for the automatic phylogenetic and functional analysis of metagenomes”. In: *BMC bioinformatics* 9.1 (2008), p. 386.
- [61] Susan K Murphy et al. “Relationship between methylome and transcriptome in patients with nonalcoholic fatty liver disease”. In: *Gastroenterology* 145.5 (2013), pp. 1076–1087.

- [62] KM Neufeld et al. “Reduced anxiety-like behavior and central neurochemical change in germ-free mice”. In: *Neurogastroenterology & Motility* 23.3 (2011), 255–e119.
- [63] Jari Oksanen et al. “The vegan package”. In: *Community ecology package* (2007), pp. 631–637.
- [64] Jason W Osborne and Anna B Costello. “Sample size and subject to item ratio in principal components analysis”. In: *Practical assessment, research & evaluation* 9.11 (2004), p. 8.
- [65] Ross Overbeek et al. “The subsystems approach to genome annotation and its use in the project to annotate 1000 genomes”. In: *Nucleic acids research* 33.17 (2005), pp. 5691–5702.
- [66] Lior Pachter. “Models for transcript quantification from RNA-Seq”. In: *arXiv preprint arXiv:1104.3889* (2011).
- [67] Javier Palarea-Albaladejo and Josep Antoni Martín-Fernández. “zCompositions—R package for multivariate imputation of left-censored data under a compositional approach”. In: *Chemometrics and Intelligent Laboratory Systems* 143 (2015), pp. 85–96.
- [68] Joseph N Paulson, Mihai Pop, and Hector Corrada Bravo. “Metastats: an improved statistical method for analysis of metagenomic data”. In: *Genome biology* 12 (2011), pp. 1–27.
- [69] Joseph Nathaniel Paulson. “metagenomeSeq: Statistical analysis for sparse high-throughput sequencing”. In: *Bioconductor package* 1 (2014).
- [70] Karl Pearson. “Mathematical Contributions to the Theory of Evolution.—On a Form of Spurious Correlation Which May Arise When Indices Are Used in the Measurement of Organs”. In: *Proceedings of the royal society of london* 60.359–367 (1896), pp. 489–498.
- [71] Elaine O Petrof et al. “Stool substitute transplant therapy for the eradication of Clostridium difficile infection:‘RePOOPulating’the gut”. In: *Microbiome* 1.1 (2013), p. 1.
- [72] David Preiss and Naveed Sattar. “Non-alcoholic fatty liver disease: an overview of prevalence, diagnosis, pathogenesis and treatment considerations”. In: *Clinical science* 115.5 (2008), pp. 141–150.
- [73] Albert Propst et al. “Prognosis and life expectancy in chronic liver disease”. In: *Digestive diseases and sciences* 40.8 (1995), pp. 1805–1815.
- [74] Christian Quast et al. “The SILVA ribosomal RNA gene database project: improved data processing and web-based tools”. In: *Nucleic acids research* 41.D1 (2013), pp. D590–D596.
- [75] Maitreyi Raman et al. “Fecal microbiome and volatile organic compound metabolome in obese humans with nonalcoholic fatty liver disease”. In: *Clinical Gastroenterology and Hepatology* 11.7 (2013), pp. 868–875.
- [76] Christian S Riesenfeld, Patrick D Schloss, and Jo Handelsman. “Metagenomics: genomic analysis of microbial communities”. In: *Annu. Rev. Genet.* 38 (2004), pp. 525–552.

- [77] Chantal A Rivera et al. “Toll-like receptor-4 signaling and Kupffer cells play pivotal roles in the pathogenesis of non-alcoholic steatohepatitis”. In: *Journal of hepatology* 47.4 (2007), pp. 571–579.
- [78] Mark D Robinson, Davis J McCarthy, and Gordon K Smyth. “edgeR: a Bioconductor package for differential expression analysis of digital gene expression data”. In: *Bioinformatics* 26.1 (2010), pp. 139–140.
- [79] Patrick D Schloss et al. “Introducing mothur: open-source, platform-independent, community-supported software for describing and comparing microbial communities”. In: *Applied and environmental microbiology* 75.23 (2009), pp. 7537–7541.
- [80] Nicola Segata et al. “Metagenomic biomarker discovery and explanation”. In: *Genome Biol* 12.6 (2011), R60.
- [81] Nicola Segata et al. “Metagenomic microbial community profiling using unique clade-specific marker genes”. In: *Nature methods* 9.8 (2012), pp. 811–814.
- [82] Ron Sender, Shai Fuchs, and Ron Milo. “Revised estimates for the number of human and bacteria cells in the body”. In: *bioRxiv* (2016), p. 036103.
- [83] Claude Elwood Shannon. “A mathematical theory of communication”. In: *ACM SIGMOBILE Mobile Computing and Communications Review* 5.1 (2001), pp. 3–55.
- [84] Daniel Simberloff. “Use of rarefaction and related methods in ecology”. In: *Biological data in water pollution assessment: quantitative and statistical analyses*. ASTM International, 1978.
- [85] Michelle I Smith et al. “Gut microbiomes of Malawian twin pairs discordant for kwashiorkor”. In: *Science* 339.6119 (2013), pp. 548–554.
- [86] Se Jin Song et al. “Cohabiting family members share microbiota with one another and with their dogs”. In: *Elife* 2 (2013), e00458.
- [87] Erica D Sonnenburg et al. “Diet-induced extinctions in the gut microbiota compound over generations”. In: *Nature* 529.7585 (2016), pp. 212–215.
- [88] Silvia Sookoian and Carlos J Pirola. “Meta-analysis of the influence of I148M variant of patatin-like phospholipase domain containing 3 gene (PNPLA3) on the susceptibility and histological severity of nonalcoholic fatty liver disease”. In: *Hepatology* 53.6 (2011), pp. 1883–1894.
- [89] Casey M Theriot et al. “Antibiotic-induced shifts in the mouse gut microbiome and metabolome increase susceptibility to Clostridium difficile infection”. In: *Nature communications* 5 (2014).
- [90] Robert Tibshirani and Guenther Walther. “Cluster validation by prediction strength”. In: *Journal of Computational and Graphical Statistics* 14.3 (2005), pp. 511–528.
- [91] Susannah G Tringe and Philip Hugenholtz. “A renaissance for the pioneering 16S rRNA gene”. In: *Current opinion in microbiology* 11.5 (2008), pp. 442–446.
- [92] Peter J Turnbaugh et al. “An obesity-associated gut microbiome with increased capacity for energy harvest”. In: *nature* 444.7122 (2006), pp. 1027–131.

- [93] Peter J Turnbaugh et al. “Diet-induced obesity is linked to marked but reversible alterations in the mouse distal gut microbiome”. In: *Cell host & microbe* 3.4 (2008), pp. 213–223.
- [94] Peter J Turnbaugh et al. “The effect of diet on the human gut microbiome: a metagenomic analysis in humanized gnotobiotic mice”. In: *Science translational medicine* 1.6 (2009), 6ra14–6ra14.
- [95] Peter J Turnbaugh et al. “The human microbiome project: exploring the microbial part of ourselves in a changing world”. In: *Nature* 449.7164 (2007), p. 804.
- [96] Camilla Urbaniak et al. “Human milk microbiota profiles in relation to birthing method, gestation and infant gender”. In: *Microbiome* 4.1 (2016), pp. 1–9.
- [97] William A Walters et al. “PrimerProspector: de novo design and taxonomic analysis of barcoded polymerase chain reaction primers”. In: *Bioinformatics* 27.8 (2011), pp. 1159–1161.
- [98] AJ Wigg et al. “The role of small intestinal bacterial overgrowth, intestinal permeability, endotoxaemia, and tumour necrosis factor  $\alpha$  in the pathogenesis of non-alcoholic steatohepatitis”. In: *Gut* 48.2 (2001), pp. 206–211.
- [99] Vincent Wai-Sun Wong et al. “Molecular characterization of the fecal microbiota in patients with nonalcoholic steatohepatitis—a longitudinal study”. In: *PLoS One* 8.4 (2013), e62885.
- [100] Mitugi Yasuda et al. “Suppressive effects of estradiol on dimethylnitrosamine-induced fibrosis of the liver in rats”. In: *Hepatology* 29.3 (1999), pp. 719–727.
- [101] Tanya Yatsunenko et al. “Human gut microbiome viewed across age and geography”. In: *Nature* 486.7402 (2012), pp. 222–227.
- [102] Lixin Zhu et al. “Characterization of gut microbiomes in nonalcoholic steatohepatitis (NASH) patients: a connection between endogenous alcohol and NASH”. In: *Hepatology* 57.2 (2013), pp. 601–609.
- [103] Marcela Zozaya-Hinchliffe et al. “Quantitative PCR assessments of bacterial species in women with and without bacterial vaginosis”. In: *Journal of clinical microbiology* 48.5 (2010), pp. 1812–1819.

# Appendix A

## Workflows

### A.1 Non-alcoholic fatty liver disease metagenomic workflow

#### A.1.1 Filter OTUs

In this experiment, the sequencing depth is expected to have the power to detect a 2 fold change up or down in bacteria that are 0.2% abundant in a sample. The OTUs were filtered to remove any with an abundance lower than 0.2% in all samples, and the OTU seed sequences were retrieved.

#### A.1.2 Get reference library genomes

The list of genomes used in the reference library was created using two sources: the Human Microbiome Project gut reference genomes (<http://hmpdacc.org/HMRGD/healthy/>), and the NCBI complete and draft bacterial genomes ([http://blast.ncbi.nlm.nih.gov/Blast.cgi?PAGE\\_TYPE=BlastSearch&BLAST\\_SPEC=MicrobialGenomes](http://blast.ncbi.nlm.nih.gov/Blast.cgi?PAGE_TYPE=BlastSearch&BLAST_SPEC=MicrobialGenomes)).

#### Human Microbiome Project

The Human Microbiome Project gut reference genomes (<http://hmpdacc.org/HMRGD/healthy/>) were all added to the reference library genome list for the metagenomic study.

#### NCBI complete and draft bacterial genomes

The draft and complete bacterial genomes can be queried here: [http://blast.ncbi.nlm.nih.gov/Blast.cgi?PAGE\\_TYPE=BlastSearch&BLAST\\_SPEC=MicrobialGenomes](http://blast.ncbi.nlm.nih.gov/Blast.cgi?PAGE_TYPE=BlastSearch&BLAST_SPEC=MicrobialGenomes). During this process, we ran into a bug using the NCBI webtool and had to search once through the wgs database, and once with Complete Genomes to get both the draft and the complete genomes.

The BLAST output can be downloaded. In this case we were only interested in the genomes that matched with 98% identity or greater. For these genomes we extracted the GI number, and performed web scraping in Python to visit <http://www.ncbi.nlm.nih.gov/nuccore/GInumber\mskip\medmuskip> and programatically retrieve the taxon ID. The taxon ID is found in [ftp://ftp.ncbi.nlm.nih.gov/genomes/ASSEMBLY\\_REPORTS/assembly\\_](ftp://ftp.ncbi.nlm.nih.gov/genomes/ASSEMBLY_REPORTS/assembly_)

`summary_genbank.txt` and the corresponding FTP link is used to download the genome. For each species found by this method, the genomes for 10 random strains are downloaded (or all of the strains if there are less than 10), to increase the coverage of the library.

### A.1.3 Get reference library coding sequences

Some of the genomes have a .gff file which includes the locations of the coding sequences already. For the rest, we used Glimmer [18] to predict open reading frames.

### A.1.4 Annotate reference library coding sequences

Annotation was performed by querying the SEED database [65] using command line BLAST (<http://www.ncbi.nlm.nih.gov/books/NBK279690/>). This is the most computationally intensive part of the process and can take a number of days, depending on your computing platform. The specific SEED database we used was downloaded June 2013, and had the fig.peg files from the 2010 SEED database which are missing from the 2013 database manually added in.

### A.1.5 Map sequenced reads to reference library

Once the sequenced reads are available, they can be mapped to the reference library using Bowtie2 [46]. Custom scripts were used to convert the mapping output to a table of counts per annotation per sample, which can then be analyzed with differential expression tools such as ALDEx2 [27].

All of the custom scripts used to perform the above for the metagenomic non-alcoholic fatty liver disease experiment can be found at [https://github.com/ruthgrace/make\\_functional\\_mapping\\_library](https://github.com/ruthgrace/make_functional_mapping_library).

# Curriculum Vitae

**Name:** Ruth Wong

**Post-Secondary Education and Degrees:** The University of Western Ontario  
London, ON  
2010-2014 B.M.Sc.

University of Western Ontario  
London, ON  
2014-2016 M.Sc.

**Honours and Awards:** Western Gold Medal  
2014

Leland Ritcey Prize  
2011

**Related Work Experience:** Summer Intern, Persistent Disk Team  
Google Inc., New York office  
Summer 2015

Google Summer of Code Participant  
Bader Lab, University of Toronto  
Summer 2014

## Publications:

Wong, Ruth G., Jia R. Wu, Gregory B. Gloor. "Expanding the UniFrac toolbox." Full length paper accepted for oral presentation at the Great Lakes Bioinformatics and the Canadian Computational Biology Conference 2016.